ABSTRACT

Title of Dissertation: THE EFFECT OF DEEP CONVECTION
ON TEMPERATURES IN THE TROPICAL TROPOPAUSE
LAYER AND ITS IMPLICATIONS TO THE REGULATION
OF TOROPICAL LOWER STRATOSPHERIC HUMIDITY

Hyun Cheol Kim, Doctor of Philosophy, 2005

Dissertation directed by: Dr. Andrew E. Dessler
Department of Meteorology

This dissertation focuses on the impact of deep convection on the thermal structure in the Tropical Tropopause Layer (TTL). Temperatures in this region play an important role in the regulation of water vapor, which in turn affects radiation, chemistry, and dynamics in the lower stratosphere. This dissertation includes two important conclusions concerning the regulation of temperature in the TTL.

First, significant cooling near the tropical tropopause is observed during the time when active convection is occurring. A composite technique is used to relate the local temperature anomalies to the evolution of local convection. Temperature profiles are measured by the Atmospheric Infrared Sounder (AIRS) onboard the *Aqua* satellite, and

the time evolution of local convections are determined by the National Centers for Environmental Protection / Aviation Weather Center (NCEP/AWS) half-hourly infrared global geostationary composite. The observations demonstrate that the TTL is cooled by convection, in agreement with previous observations and model simulations. By using a global data set, the variations in this convective cooling are investigated by season and region. The estimated cooling rate during active convection is - 7 K/day. This exceeds the likely contribution from cloud-top radiative cooling, suggesting turbulent mixing of deep convection plays a role in cooling the TTL.

Second, height and thermal structure of the overshooting deep convection in the TTL are investigated using visible and infrared observations from the Visible and Infrared Scanner (VIRS) onboard the Tropical Rainfall Measuring Mission (TRMM) satellite. The heights of overshooting clouds are estimated from the sizes of the visible shadows that these clouds cast. The temperature information is obtained from the mid-infrared channel. From these, the lapse rate in the cloud is estimated. The result shows that the measured lapse rate of these clouds is significantly below adiabatic. Mixing between these clouds and the near-tropopause environment is the most likely explanation. As a result, these clouds will likely settle at a final altitude above the convections' initial level of neutral buoyancy.

The Effect of Deep Convection on Temperatures in the Tropical Tropopause Layer and Its Implications to the Regulation of Tropical Lower Stratospheric Humidity

by

Hyun Cheol Kim

Thesis submitted to the Faculty of the Graduate School of the
University of Maryland, College Park in partial fulfillment
of the requirements for the degree of
Doctor of Philosophy
2005

Advisory Committee:
Professor Robert Hudson, Chair
Professor Sumant Nigam
Professor Sung W. Lee
Professor Daniel Kirk-Davidoff
Dr. Andrew E. Dessler, Advisor

ACKNOWLEDGMENTS

I foremost would like to thank my advisor, Andrew Dessler, for his patience, encouragement, and guidance. I also would like to thank Drs. Robert Hudson, Sumant Nigam, Daniel Kirk-Davidoff, and Sung Won Lee for serving as committee members and for their suggestions for improving this thesis.

Thanks also to Sun, Likun, and Emily for their supports and helpful discussions.

Finally, I would like to thank my family and my wife, Ji-Yeon, for all the support and assurances that they have given me.

TABLE OF CONTENTS

LIST OF TABLES

LIST OF FIGURES

Chapter 1. Background

1.1 Motivation

The goal of this research is to explore the role of deep convection in the regulation of temperatures near the tropical tropopause. This region's thermal structure, especially the coldest temperature, is highly associated with the regulation of water vapor in the upper troposphere and the lower stratosphere. Low-latitude water vapor at these levels is important not only for its greenhouse forcing, but also because the air here is transported into the stratosphere, where water vapor plays an important role in stratospheric chemistry, dynamics and radiation [SPARC, 2000].

It is well agreed that convection plays an important role in the regulation of the lower and middle tropospheric temperature profile. However, there is still no consensus on whether the effect of convective events can reach up to the tropopause level. The motivation of this dissertation stems from this question: whether deep convection can affect properties in the region near the tropical tropopause. Especially, this study focuses on the role of overshooting deep convection that penetrates into this region.

This dissertation includes two studies on the effects of convection in the region, which is referred to as the tropical tropopause layer (TTL). First, chapter 2 demonstrates that cooling at the tropical tropopause is observed during times when active convection occurs below. The possible role of overshooting deep convection in contributing to this observed cooling is discussed. Second, chapter 3 investigates the features of overshooting deep convection that penetrates into the TTL, such as how high deep convection overshoots, and whether this overshot air can remain in the higher level.

Background to these questions is reviewed in chapter 1. This chapter discusses the definition of the TTL, the relation between the temperature and water vapor mixing ratio in the TTL, and theories to explain regulation of the tropical lower stratospheric humidity.

1.2 The tropical tropopause layer (TTL)

1.2.1 Description of the tropical tropopause layer

In the Tropics, the troposphere is the layer of the atmosphere that extends from the earth's surface to an altitude of approximately 16 km. It is characterized by convective overturning which is driven by surface heating. Temperature generally decreases with altitude with a global mean lapse rate of approximately 6.5 K/km. Above the troposphere, there is a layer referred to as the stratosphere where ozone heating causes the temperature to increase with altitude. In the stratosphere there are

only weak vertical motions, and this layer is dominated by radiative processes. The interface between the troposphere and the stratosphere is referred to as the tropopause. There exist several definitions of the tropical tropopause, but no consensus has been reached yet on the exact definition [Highwood and Hoskins, 1998].

Furthermore, recent research has shown that the transition from the troposphere to stratosphere in the tropics should be understood as a gradual one rather than a sudden change at a sharp material boundary [Highwood and Hoskins, 1998; Sherwood and Dessler, 2000; Thuburn and Craig, 2002]. The concept of a tropical tropopause 'layer' dates back to Newton and Persson [1962]. They pointed out the existence of a "secondary tropical tropopause" well below the main tropopause. Atticks and Robinson [1983] also suggested the tropical tropopause as a "transition layer" between about 140 and 60 mb instead of a discrete boundary.

Sherwood and Dessler [2000, 2001] called this transition region the Tropical Tropopause Layer (TTL), which is defined as the region of the tropical atmosphere extending from the zero net radiative heating level (355K, 150 hPa, 14 km) to the highest level that convection reaches (~420 – 450 K, 70 hPa, 18 - 20 km). The TTL can be thought of as a transition layer between the troposphere and stratosphere, having characteristics of both regions. This study uses the same definition of the TTL as that used by Sherwood and Dessler [2000,2001].

Below the bottom of the TTL, the clear sky radiation shows net radiative cooling [Folkins, 2002], and this radiative cooling is balanced by the latent heating through convection. Above the top of the TTL, net radiative heating balances the upwelling

forces from the stratosphere by wave driven stratospheric pumping [Holton et al., 1995]. In the TTL, radiative heating balances the cooling by the mixing of overshooting cumulus clouds and the downward extension of the Brewer-Dobson circulation. However, the relative amount of their contribution is not clear.

1.2.2 Convective impact in the TTL

No common agreement has yet been reached on what role convection plays in setting temperatures near the tropical tropopause, especially near the cold point. In this region, both convective and radiative effects control the temperature profile [Held, 1982]. In the classical point of view, the tropical cold point has been considered as a division between convective and radiative control of the temperature sounding.

It is clear that the thermal structure is maintained by convection in the lower and middle troposphere, where the lapse rate is very close to the moist adiabat. However, in the upper troposphere, the temperature profile deviates substantially from the moist adiabat, so it is hard to verify the convective impact in this region. The question is whether convective impact can reach up to the tropical tropopause and affect properties in the region, such as temperature and humidity. Recent studies, based on a one-dimensional radiative convective equilibrium model, suggest that the cold point in the temperature profile is actually a stratospheric feature that has nothing to do with convection [Kirk-Davidoff et al., 1999; Thuburn and Craig, 2002]. Thuburn and Craig [2002] showed that a temperature minimum in radiative equilibrium can exist well

above the convectively adjusted region, suggesting no direct role of convection on the cold point temperature.

A variety of observational evidence, however, suggests the tropopause temperatures are indeed affected by tropospheric processes [Johnson and Kriete, 1982; Highwood and Hoskins, 1998; Sherwood et al., 2003]. A climatological connection between tropopause temperatures and convection has also been shown [Reid and Gage, 1981; Reid and Gage, 1985; Randel et al., 2000]. Randel et al. [2000] showed that variations in tropopause characteristics are coherent with the El Nino-Southern Oscillation (ENSO). Kiladis et al. [2001] also showed the tropopause potential temperature over a site in the western Pacific changes in response to the movement of convection.

1.2.3 Overshooting deep convection into the TTL

One of the most efficient ways for deep convection to affect properties in the TTL is by mixing-in of the overshooting deep convection into the air in the TTL. The equivalent potential temperature in the boundary layer of convective regions peaks at 345 K and is generally less than ~355 – 360 K [Folkins et al., 2000]. 'Overshooting' deep convection describes convection reaching potential temperatures higher than ~355 – 360 K, and that has likely overshot its level of neutral buoyancy (LNB). If this air subsequently mixes with higher potential temperature air during 'overshooting', the resulting mixture will settle at altitudes above the parcel's initial LNB.

Figure 1.1 describes the impact of convection mixing into the environmental air in the upper troposphere and the TTL. Below the LNB, which is usually located near 14 km, the temperature in a convective cloud that generated in the boundary layer is usually warmer than the environmental air. Above the LNB, an overshooting cloud still follows the moist adiabat, and its temperature is much colder than that of the environment. If this convection mixes with air at levels higher than the LNB, it can have a significant cooling effect on the environmental air.

Observations show overshooting deep convective clouds do penetrate into the TTL [Danielsen, 1982], but there is doubt that they occur in sufficient abundance to account for substantial cooling in the TTL [Gettelman et al. 2002]. In order to characterize this cooling mechanism, it is necessary to investigate the heights of overshooting clouds and efficiency of mixing during the overshooting.

The most common method of measuring cloud heights is from thermal brightness temperatures [Gettelman et al., 2002]. With this method, the cloud top height for a deep convective cloud, which is optically thick, is obtained by observing its effective blackbody temperature (brightness temperature) at some wavelength (~ 11- μm) and matching this to a local atmospheric sounding. There is, however, an uncertainty in the conversion from brightness temperature to cloud-top height [e. g. Sherwood et al., 2004]. In this study, an alternative method is used to determine the height of overshooting deep convective clouds.

If convection affects properties near the tropical tropopause, there are important implications for the dehydration of air masses entering the tropical lower stratosphere.

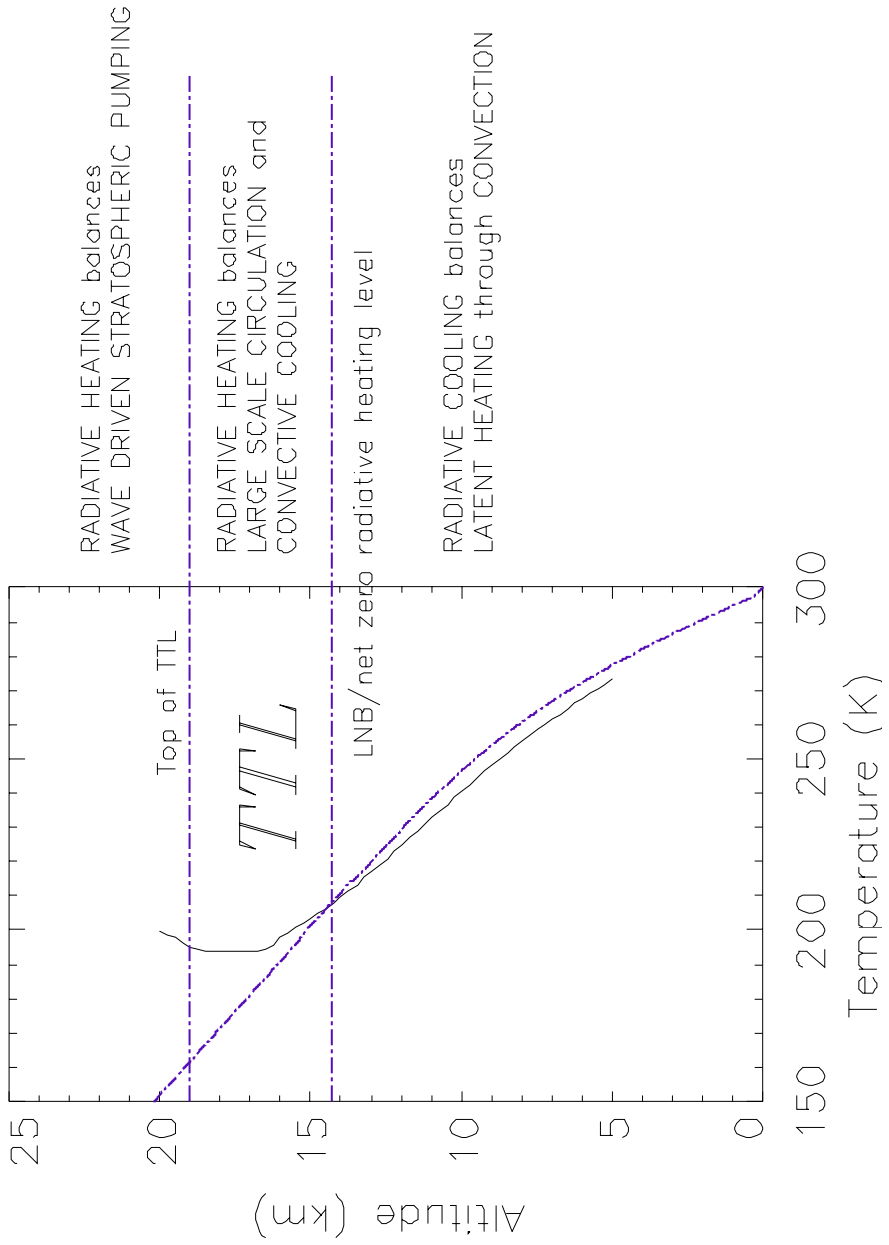

Figure 1.1 Convective impact in the TTL. The solid line shows the mean temperature profile in the tropics; The dashed line shows the adiabat. Air in the undiluted overshooting convective cloud follows the moist adiabat, so its temperature is colder than that of the environment in the TTL.

Detrained air from convective clouds that deeply penetrate near the tropical tropopause is not only very cold, but also very dry, and has great potential to supply dehydrated air into the TTL. Detailed discussion on the convective impact on water vapor regulation in the TTL is introduced in the next section.

1.3 Water vapor in the TTL

1.3.1 Effects of water vapor

The principal impact of water vapor on the radiative balance in the region near the tropical tropopause, the upper troposphere (UT), and the lower stratosphere (LS), is through the long-wave, infrared part of the spectrum. H_2O has a non-linear, asymmetric molecule with a large permanent dipole moment. It has a pure rotation spectrum centered at 20 μm and a strong ν2 vibration-rotation band centered at 6.3 μm [Goody, 1964]. In addition, water vapor exhibits a continuum absorption across a wide range of the infrared spectrum, being most noticeable in the 'window' region between about 800 and 1250 cm^{-1} (12.5 – 8.0 μm) [Bignell, 1970; Burch, 1981]. Because of the strong absorption and emission in these bands, water vapor is the dominant greenhouse gas in the atmosphere.

In the stratosphere, the humidity is extremely low: mixing ratios of a few parts per million are typical. Even so, the radiative effects of stratospheric water vapor are significant [Goody, 1964; Forster and Shine, 1999; Shindell, 2001]. Forster and Shine (1999) showed that the increasing trend of stratospheric water vapor could have led to

a cooling of the mid- and high-latitude lower stratosphere in excess of 1.0K, which is comparable to that caused by the stratospheric ozone losses. Using the Goddard Institute for Space Studies (GISS) climate model, Shindell [2001] demonstrated that stratospheric water vapor abundance could affect ozone, surface climate, and stratospheric temperatures. Evidence has been accumulating over many years [Oltmans and Hofmann, 1995; Evans et al., 1998] that H_2O mixing ratios in the lower stratosphere may be increasing with time. Therefore, understanding the radiative impact of such changes is very important in the context of future climate change.

Water vapor is also important for chemistry of the UT/LS. It is the source of the hydroxyl radical (OH) in both the troposphere and the stratosphere. OH is of direct importance in many chemical cycles in both regions [Brasseur and Solomon, 1984; Wayne, 1985]. HOx (= OH + HO_2) radicals take part in important catalytic cycles which regulate the production and destruction of ozone in both the troposphere and stratosphere [Wennberg et al., 1994]. A stratospheric water vapor increase leads to an increased OH concentration, which results primarily in an enhanced ozone depletion by the HOx-cycle. A long-term increase in stratospheric water vapor affects the heterogeneous ozone destruction (ClOx-cycle) within the Antarctic polar vortex that is caused by an enhanced formation of polar stratospheric clouds (PSCs) [Stenke and Grewe, 2004].

OH also controls the oxidizing capacity of the atmosphere for short-lived gases, and regulates the lifetimes of the longer-lived species such as CO and CH_4. Thus, it is important to understand the dynamics driving the concentration and distribution of

water vapor, as well as the chemical and photochemical reactions that transform water vapor into OH.

1.3.2 Water vapor and cold point temperature

Based on the data measured by frost-point hygrometer from the British Meteorological Research Flight (MRF) over Southern England, Brewer [1949] inferred the general feature of the stratospheric circulation. He found that the tropopause frost-point temperature is –58 °C (~55 ppmv near 250 hPa), while the mixing ratio 2 km above the tropopause is as low as 1.6 ppmv. He explained the observed extreme dryness of the stratosphere by arguing that nearly all air parcels entering the stratosphere must cross the tropopause in the tropics, where they experience freeze-drying to the saturation mixing ratio characteristic of the cold tropical tropopause. He argued that this ascent is a part of a global-scale circulation, which was later called the Brewer-Dobson circulation. In the Brewer-Dobson circulation, air slowly ascends in the tropical troposphere into the stratosphere through the tropical tropopause, then moves pole-ward, and finally descends back to the troposphere in the mid-latitude region.

His idea was supported by the so-called “tape recorder effect”. The freeze-drying hypothesis implies that water vapor mixing ratios of air entering the tropical stratosphere should vary seasonally in phase with the annual cycle of the tropical tropopause temperature. Thus, just as a signal is recorded on a magnetic tape as it

passes the head of a tape recorder, the minimum saturation mixing ratio near the tropical tropopause should be recorded on each layer of air moving upward in the large-scale tropical stratospheric circulation. This effect was confirmed by various observations [Mote et al., 1995; 1996].

However, there are still unanswered questions on the relation of lower stratospheric water vapor and cold point temperature. First, the observed stratospheric water vapor mixing ratios are less than saturation at the mean tropopause temperature. Second, the trend in stratospheric water vapor is positive, but the trend in tropical tropopause temperature is negative.

Water vapor entry level and saturation mixing ratio: Early observation [Kley et al., 1979; Jones et al., 1986] showed that air entering the tropical stratosphere was drier than that predicted by freeze-drying at the zonal-mean tropopause temperature. Kley et al. [1979] used data from four balloon flights of the NOAA ultraviolet fluorescence stratospheric water vapor instrument, and showed that the minimum water vapor mixing ratio occurs 2 - 3 km above the tropopause in both the tropics and midlatitudes. Measured minimum values were 2.6 ppmv over Brazil (5S) and 3.6 ppmv over Wyoming (41N), with an estimated total error of 20%. This is much drier than that expected from the tropopause temperature, 5-6 ppmv, which is estimated from the typical temperature of the tropical tropopause.

There are only two known sources for stratospheric water vapor. One process to generate stratospheric H_2O, which is also responsible for the increase of the water

vapor mixing ratio with altitude in the stratosphere, is photochemical CH_4 oxidation [Brasseur and Solomon, 1984; Letexier et al., 1988]. Oxidation of each CH_4 molecule in the lower and mid stratosphere creates about 2 H_2O molecules [Jones et al., 1986]. Otherwise, stratospheric H_2O is transported from the troposphere through the tropical tropopause.

Due to many technical difficulties, it is not easy to measure directly the amount of $[H_2O]_e$, the entry level of water vapor to the stratosphere. Instead, simultaneous measurements of CH_4 and H_2O in the extratropics are used to estimate the entry amount of water vapor through the topical tropopause. First, measurements of CH_4 in the extratropical stratosphere are used to determine how much of the water vapor in these regions was produced in the stratosphere. Subtracting this from the mid-latitude H_2O abundance yields an estimate for $[H_2O]_e$.

Table 1.1 shows a list of estimates of $[H_2O]_e$ from various instruments. Estimates are from 2.7 ppmv to 4.2 ppmv, mostly ranging between 3.6 ppmv and 3.8 ppmv. For the same period, the saturation mixing ratios of water vapor at the tropical cold point temperature are clearly over 4 ppmv [Zhou et al., 2001], suggesting additional mechanisms for the hydration of the lower stratosphere.

Trend: Observations indicate rising concentrations of stratospheric water vapor [Oltmans and Hofmann, 1995; Abbas et al., 1996; Evans et al., 1998; Nedoluha et al., 1998; Michelsen et al., 2000; Oltmans et al. 2000]. Oltmans et al. [2000] used data from frostpoint hydrometer measurements at Washington, D.C. and Boulder, to show

that water vapor concentrations have increased at a rate of 1 – 1.5 %/yr (0.05 – 0.07 ppmv/yr) for the past several decades. There has been a 2 ppmv increase of stratospheric water vapor since the middle 1950s [SPARC, 2000]. This is a substantial number, given the typical current stratospheric values of 4-6 ppmv. The increase in the concentration of tropospheric methane since the 1950s (0.55 ppmv) is responsible for at most one half of the increase in stratospheric water vapor over this time period [Oltmans et al., 2000]. It is not clear what mechanisms are responsible for the remainder of the observed increase in stratospheric water vapor.

The change of temperature at the tropical tropopause, however, shows a different trend from that of lower stratospheric water vapor. Using data produced operationally by the European Centre for Medium-Range Weather Forecasts (ECMWF), Simmons et al. [1999] showed a cooling trend of about 0.6º per decade from the global means of the 100 hPa temperature analyses. Zhou et al. [2001] also showed a trend of cold point tropopause (CPT). They used data from the operational daily rawinsonde from stations between 10º S and 10º N from 1973 to 1998, and showed a cooling trend of -0.57 ± 0.06 K/decade in the corresponding period.

This discrepancy between the trends of lower stratospheric water vapor and cold tropopause temperature implies that there must be other, more complicated dehydration processes occurring during the tropical stratosphere-troposphere exchange. In the next section, theories to explain the dryness of the lower stratosphere are discussed.

Instrument	$[H_2O]_e$ (ppmv)	Period	Reference	SMR (ppmv) (Zhou et al. 2001)
LMS	2.7 ± 0.35	1979	Jones et al. [1986]	4.92
LMS	3.3 ± 0.2	1979	Hansen and Robinson [1989]	4.92
SAGE II	2.9 (2.3-3.5)	1981-91	Chiou et al. [1997]	
MLS	3.0 ± 0.27	1992-93	SPARC [2000]	
LMD	3.61 ± 0.28	1991-92	Engel et al. [1996]	4.41
WVMS	3.6 ± 0.5	1992-97	SPARC [2000]	
ATMOS	3.6 ± 0.5	1985-94	SPARC [2000]	
ATMOS	3.5 ± 0.3	1985-94	Michelsen et al. [2000]	
FIRS-2	3.6 ± 0.4	1989-97	SPARC [2000]	
POAM-III	3.4 ± 0.4 (NH) 4.0 ± 0.5 (SH)	1998-99	SPARC [2000]	
HALOE ver. 19	3.8 ± 0.49	1993-97	Dessler and Kim [1999]	4.13
HALOE ver. 19	3.6 ± 0.2	1993-2000	SPARC [2000]	
FISH	3.9 ± 1.0	Sep. 1993	Zőger et al. [1999]	4.38
MkIV	3.8 ± 0.2	1990-97	SPARC [2000]	
CMDL	3.8 ± 0.6	1996-98	SPARC [2000]	
MAS	3.8 ± 0.5	1992-94	SPARC [2000]	
MIPAS	3.85 ± 0.2	Feb. 1995	Stowasser et al. [1999]	
MIPAS	3.88 ± 0.1	Mar. 1997	Stowasser et al. [1999]	
NOAA Ly-α	4.0 ± 0.4	1993-95	Hurst et al. [1999]	
NOAA Ly-α	3.7 – 4.2	1987-89	Kelly et al. [1990]	4.30
NOAA Ly-α	3.9 ± 0.1	May 1998	SPARC [2000]	
JPL TDL	3.9 ± 0.3	1997	Hurst et al. [1999]	
Harvard Ly- α	4.1 ± 0.3	1993-99	Hurst et al. [1999]	

Table 1.1 Estimates of water vapor entering the stratosphere ($[H_2O]_e$). Saturation mixing ratios (SMRs) of water vapor at the tropical cold point temperature (CPT) are listed in column 5.

1.4 Theories of stratospheric dehydration

1.4.1 Slow dehydration

There are several theories to explain the extreme dryness of the lower stratosphere. Brewer [1949] suggested a circulation model in which air enters into the stratosphere through the cold tropical tropopause, dehydrating the air by freeze-drying. However, his explanation is not enough because the observed stratospheric water vapor mixing ratios are much less than saturation at the mean tropopause temperature.

Extending this model, Newell and Gould-Stewart [1981] proposed the so-called "staratospheric fountain" theory, which postulates that air enters the stratosphere preferentially at the times and in the locations with the coldest tropopause temperature. Based on an analysis of global 100 hPa monthly mean temperatures, they argued that the major air mass entry into the stratosphere occurs over the western tropical Pacific, northern Australia, Indonesia, and Malaysia in the November-March period and over the Bay of Bengal and India during the Monsoon. By showing the mean mass flux in the fountain region yields upwelling motion, they suggested that this mean large-scale ascent is responsible for the transport and subsequent dehydration of air entering the stratosphere.

However, this slow dehydration mechanism by mean large-scale ascending motion has been brought into question. Robinson [1980] noted that such gradual, uniform ascent would make the tropical upper troposphere saturated and cloudy, causing extensive cloud shields over tropical area. Winker and Trepte [1998] showed

that recent lidar images of thin cirrus clouds have about 20 % coverage distributed widely through the Tropics; these clouds also occur at a variety of altitudes, and not generally right at the tropopause. Sherwood [2000] also showed that air is sinking out of the stratosphere in the regions where the tropopause is coldest, suggesting a diabatic cooling occurs in these regions.

Another mechanism that can cause slow dehydration is in situ dehydration over meso- or synoptic-scale convective systems. Adiabatic lifting by these systems can raise the lower stratosphere, producing substantial cooling in some cases [e.g., Fritsch and Brown, 1982]. If these systems persist for up to several days, condensation and removal of significant amounts of vapor can occur.

Cooling also occurs by wave activities near the tropopause [Pfister, 1986; Tsuda et al., 1994; Alexander and Pfister, 1995; Potter and Holton, 1995; Jensen et al., 1996; Boehm and Verlinde, 2000]. Using a mesoscale dynamical model of tropical convection, Potter and Holton [1995] demonstrated that the generation of stratospheric buoyancy waves and wave clouds by tropical convection may be responsible for the minimum water vapor mixing ratio observed a few kilometers over the tropical tropopause. Boehm and Verlinde [2000] also showed that uplift associated with Kelvin waves, convectively generated gravity waves, or forced circulations associated with organized convective systems can cause an adiabatic cooling of air parcels near the tropical tropopause, generating sub-visible cirrus clouds.

1.4.2 Rapid dehydration

An alternative dehydration mechanism is vigorous convection, originating near the surface, overshooting the tropopause, and mixing with stratospheric air, thereby transferring mass from the troposphere directly into the stratosphere [Danielsen, 1982; 1993]. Danielsen [1982] discussed the role of large cumulonimbus that penetrate the stratosphere and form huge anvils in the lower stratosphere, suggesting a radiative heating at the anvil base combined with cooling at the anvil top drives a dehydrating mechanism. Radiative heating at the base of the cumulonimbus would lead to subsaturated air, while radiative cooling at the top of the anvil would lead to supersaturated air. The supersaturated air at the top of the anvil would lead to a rapid growth of ice crystals, which could then precipitate, dehydrating the anvil region.

This idea was supported by observational evidence. Several cases of very cold overshoots have been reported [Adler and Mack, 1986; Ebert and Holland, 1992; Simpson et al., 1998]. Observations by the Water Vapor Exchange Experiment (WVEE) at Panama and Darwin demonstrated the existence of overshooting clouds that penetrate into the stratosphere and mix tropospheric and stratospheric air together [Danielsen, 1982]. The potential temperature of the resulting mixture is over 380 K, a higher value than the maximum observed tropospheric equivalent potential temperature of 367 K [Selkirk, 1993]. Particle measurements by Knollenberg et al. [1982] also showed bigger ice crystal sizes in the anvil, implying the ice would fall out quickly, without re-evaporation. The tropical experiment of the Stratosphere-

Troposphere Exchange Project (STEP/Tropical) showed the same result as in WVEE, observing tropospheric air penetrating and mixing into the stratospheric air.

It seems clear that penetrative overshooting clouds do exist. However, the question of their frequency, i. e. whether this kind of overshooting occurs often enough to generate significant dehydration, is still unanswered. Recent work suggests that tropical convection is generally capped at altitudes 2-4 km below the tropical cold-point tropopause, so there is only infrequent penetrative overshooting that reaches to the tropical tropopause level [Highwood and Hoskins, 1998; Folkins et al., 1999; Keith, 2000; Gettelman et al., 2001].

Sherwood and Dessler [2000, 2001] extended this convective dehydration hypothesis, and suggested a dehydration model by convective detrainment mixing into the TTL. In this TTL hypothesis, air is dehydrated rapidly as suggested by Danielsen [1982] but detrains at variable levels throughout the depth of the TTL. The bottom of the TTL is close to the typical level of neutral buoyancy (LNB) of tropical convection [Selkirk, 1993]. Air detraining near the bottom of the TTL will have typical values of water vapor mixing ratio (10-15 ppmv), which is relatively moist compared to the stratosphere. Air detraining at higher altitudes, however, must have originated in more energetic and warmer updrafts and/or overshot significantly. This air can be dehydrated to moisture levels far below average for the TTL.

This newly dehydrated air, provided by overshooting clouds, spreads horizontally from the convective region, then mixes with moister air that detrained earlier at lower altitudes and has slowly risen to this altitude. Air on any given θ

surface will therefore have a vapor level weighted between newly dehydrated air by rapid uplift and rather older air that has slowly risen all the way from the bottom of the TTL. At locations farther from intense convection, this mixing will be weighted more toward older air, causing mean vapor levels to be greater.

Convection plays a very important role in this hypothesis, but existing detailed study on the features of overshooting convection is not sufficient. In this study, I will explore the feasibility of this hypothesis, especially the height of overshooting convective clouds and the mixing process during overshooting.

1.5 Conclusion and dissertation overview

This study focuses on the effect of convection on the properties of the TTL, especially temperature and humidity. The regulation of water vapor in the TTL is strongly associated with the shaping of the region's thermal structure. Water vapor in the TTL is important because it has a significant radiative and chemical effect in this region. As well, it is an important tracer gas, allowing us to see the transport of air mass from the tropical troposphere into the tropical stratosphere.

Rapid dehydration by convective overshooting clouds is one of the suggested hypotheses to explain the dryness of the tropical lower stratosphere. Studying characteristics of deep convection that penetrates into the TTL is important to explain the feasibility of the convective dehydration mechanism, and is a main goal of this study. This study will demonstrate:

1. Observation of tropopause cooling during active deep convection.

2. Measurements of overshooting deep convective cloud heights.

3. Mixing of overshooting cloud into the environmental air.

In chapter 2, the effect of convection on the temperature profile in the TTL is investigated, using a composite technique that relates the change of temperature profile and the growth of local convection. Using temperature profiles measured by the Atmospheric Infrared Sounder (AIRS) onboard the *Aqua* satellite, and the time evolution of local convection determined by the National Centers for Environmental Protection / Aviation Weather Center (NCEP/AWS) half-hourly infrared global geostationary composite, analysis shows a clear signal that the TTL is cooled by convection. Cooling rate calculations were also performed to see how fast this cooling occurs.

In chapter 3, the height of overshooting clouds was inferred from the size of the visible shadows that these clouds cast, and temperature information was obtained from the mid-infrared channel. From this, the lapse rate in the cloud in the upper troposphere is estimated. Moreover, a possible process to explain this thermal structure is discussed.

Finally, a summary and conclusions are presented in chapter 4.

Chapter 2. Observations of convective cooling in the tropical tropopause layer in AIRS data

2.1 Introduction

Though it is well known that convection plays an important role in regulating the thermal structure of the tropical troposphere, its effect on temperatures in the transition region between the tropical troposphere and stratosphere still remains unclear. On the one hand, only a small fraction of convection extends to the vicinity of the tropical tropopause [Gettelman et al., 2002]; on the other, there is no reason to suppose that infrequent events cannot still have an effect. The question of how such infrequent deep convection affects this region's temperature is of great interest for many reasons, including the role this region's temperature plays in controlling lower stratospheric humidity [SPARC, 2000].

Various observational evidence suggests that tropopause temperatures are affected by convection. Using rawinsonde data during the International Winter Monsoon Experiment (Winter MONEX), Johnson and Kriete [1982] demonstrated that a significant cold anomaly occurs above the top of the mesoscale anvil clouds in the Indonesia region. Sherwood et al. [2003] used an 18-month set of radiosonde data from the tropical western Pacific region, and showed that active convective systems

are locally associated with cold anomalies in the lower troposphere and near the tropopause. Using a dry baroclinic model with imposed idealized tropical convective heating, Highwood and Hoskins [1998] demonstrated that tropopause properties are directly related to the large-scale convective heating occurring below. Randel et al. [2003] also showed that there is a strong correlation between cold temperature anomaly near the tropical tropopause and low outgoing long wave radiation data (a proxy for tropical deep convection) by analyzing data from Global Positioning System Meteorology (GPS/MET) observations. A cloud-resolving model by Kuang and Bretherton [2004] also showed that convection has a cooling effect in the TTL.

Johnson and Kriete [1982] suggested adiabatic lifting, cloud-top radiative cooling, or turbulent mixing could explain the tropopause cooling. They also argued that the amount of very high and deep clouds may not be sufficient to cause appropriate cloud-top radiative cooling. Hartmann et al. [2001], however, showed that, if thin tropical tropopause cirrus ($\tau << 1$) lies above convective anvils with tops above 13 km, net radiative cooling from the cirrus could cause cooling. Wave propagation induced by diabatic heating in the troposphere also can contribute to cooling near the tropopause [Randel et al., 2003; Sherwood et al., 2003]. Sherwood et al. [2003] argued that this cooling is induced by diabatic process and likely caused by mixing of cold air that detrains from overshooting deep convection with its environment [Sherwood, 2000].

To study the response of the tropopause temperature to the convective events below, Sherwood et al. [2003] used a compositing technique that relates the temporal

progression of tropical convective systems and the temperature changes in their vicinity. In this study, the work of Sherwood et al. [2003] is extended by using a new, global dataset. The magnitude of the convective cooling is investigated as a function of location and season. The cooling rate due to convection is also calculated, which will help us narrow down the possible causes of the cooling.

2.2 Data & Methodology

In order to observe the effects of convection on the thermal structure of the TTL, we need to take temperature measurements and sort them according to their "convective stage." I use temperature soundings measured by the Atmospheric Infrared Sounder (AIRS, onboard the Aqua spacecraft), obtained during February and July 2003 and between 30°N and 30°S. AIRS level 2 products provide near-global temperature soundings twice a day with 50-km horizontal resolution, at an accuracy of 1°C in layers 1-km thick [Susskind et al., 1998]. For the data we used in this study, version 3.0.8.0, retrievals are done only if the surface type is water, so this study is limited to areas over ocean only.

I assign a "convective stage" to each AIRS temperature sounding using the National Centers for Environmental Protection / Aviation Weather Center (NCEP/AWS) infrared global geostationary composite (hereafter the IR imagery), archived at the Global Hydrology Resource Center (GHRC). This IR imagery dataset contains images of the brightness temperature (T_b) converted from the 11-μm infrared

channels of four weather satellites in geosynchronous orbit, with 14-km horizontal resolution and half hourly temporal resolution. These satellites are the Geostationary Meteorological Satellite (GMS, Japan), Geostationary Operational Environmental Satellites-East (GOES-East), GOES-West (USA), and Meteosat (Europe), which cover the whole globe except for a very narrow gap over the Indian Ocean [Kidder and Vonder Haar, 1995].

In order to determine what "convective stage" applies to a particular AIRS sounding, I first determine the time history of convection in every 1°x1° box. I define convection as "occurring" during a 30-minute period if the fraction of pixels in a box with brightness temperatures below 208 K (C_{208}) is greater than 10% (this is the same threshold as used by Sherwood and Wahrlich [1999]); it is not occurring if $C_{208} < 10\%$. Using this method, I determine when convection starts and stops for each 1°x1° box.

For each AIRS temperature profile, I look within ±3 hours of the profiles' measurement time and determine the time history of convection in the 1°x1° box around the measurement. Each sounding is assigned according to its stage of convective development. The six stages of development are defined in Table 2.1.

An example of convective stage determination is shown in Fig. 2.1. The thick solid line shows the change of C_{208} measured at 180ºE, 10ºS during 10 Feb. 2003 – 11 Feb. 2003. Hours after 00Z 10 Feb. 2003 are shown in x-axis. Convection begins at 15h 30m when C_{208} becomes over 10 % (the horizontal dashed line), and ends at 27h (3Z Feb. 11, 2003). The total duration of this convection is 11 hours 30 minutes. Assigned convective stage numbers are shown at the bottom. It should be noted that

Stages	Condition
0	No convection within ±3 hours
1	No convection in the previous 3 hours, convection starts in the next 3 hours
2	Convection started in the previous 3 hours and continues for the next 3 hours
3	On going $C_{208} > 10\%$ for the entire 6-hour period
4	Convection on-going during previous 3 hours, convection stops in the next 3 hours
5	Convection stopped in the previous 3 hours, no convection in the next 3 hours

Table 2.1 Stages of convective development

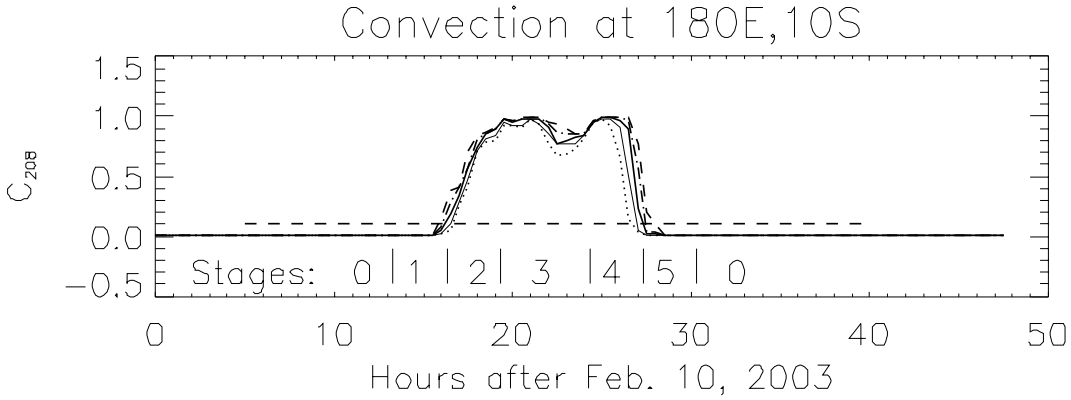

Figure 2.1 An example of convective stage determination. The thick line shows C_{208} (the fraction of pixels in a box with brightness temperatures below 208 K) measured at 180ºE, 10ºS Feb. 10, 2003. Convection is determined as "occurring" if C_{208} is over 10 % (horizontal dashed line). C_{204}, C_{206}, C_{210}, and C_{212} are shown as dotted, dashed, dot-dashed, and thin line. Determined convective stages are shown at the bottom.

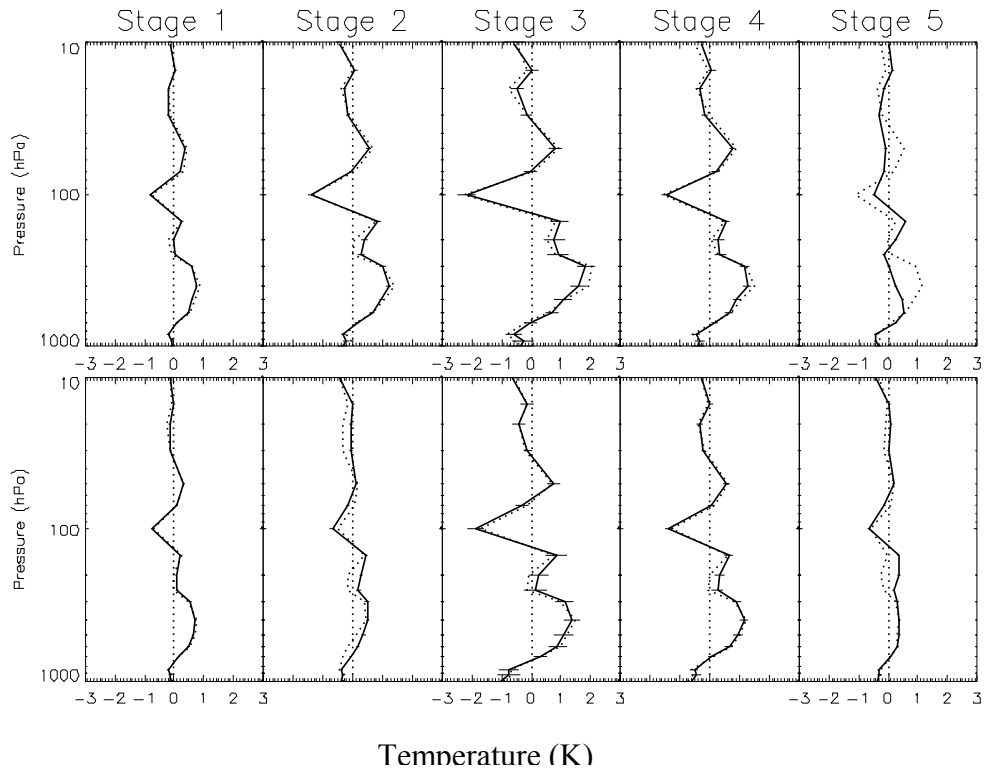

Figure 2.2 Mean temperature anomaly over convective stages for (a) Feb. 2003 and (b) Jul. 2003. Dotted lines indicate values from nighttime only. Horizontal bars at each pressure level mean the 95% confidence interval for mean of the temperature anomaly.

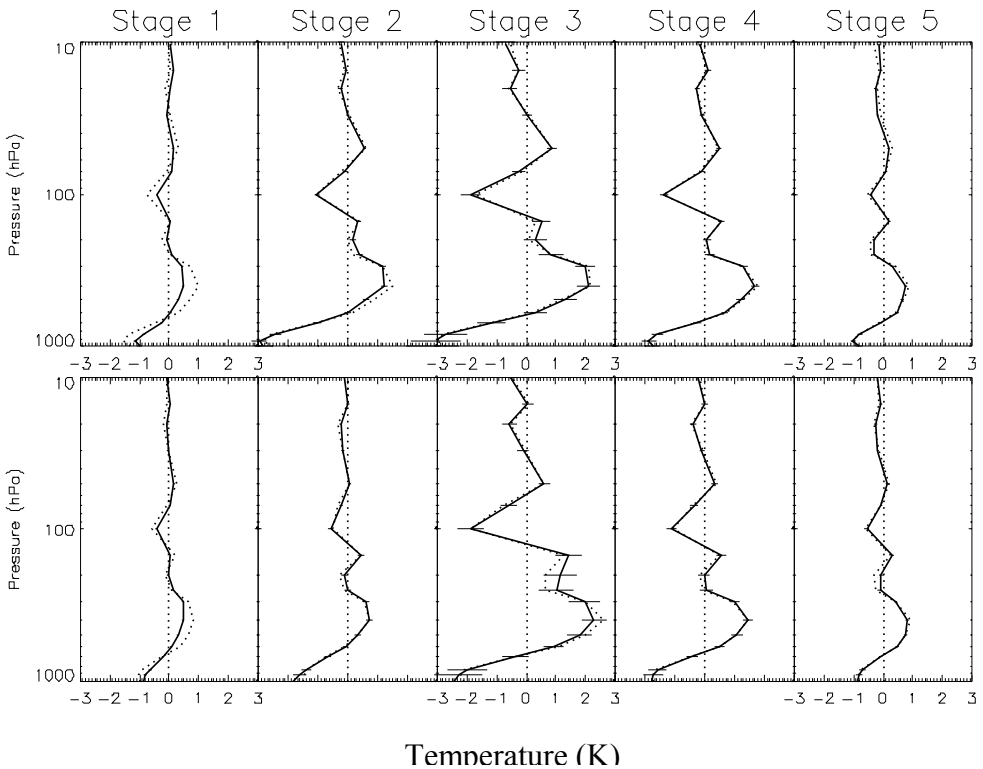

Figure 2.3 Same with Fig.2.2 but data over land.

the duration of stage 1, 2, 4, and 5 is always 3 hours, but the duration of stage 3 varies according to the total duration of convection. We also showed different temperature thresholds: C_{204} (dotted), C_{206} (dashed), C_{210} (dot-dashed), and C_{212} (thin line). It should be noted that the change of temperature threshold barely affects the convective stage determination, while the change of fractional threshold, 10%, has some effects on the determination of convective stages.

In addition, the advection of clouds is not considered here. Therefore, it is not possible to distinguish a system moving in from one that grows locally. I also throw out any measurement whose convective history does not fall into one of those categories. For example, convection that lasts shorter than 6 hours does not fall into any category and therefore is not analyzed here.

2.3 Results

2.3.1 Temperature anomaly

Figures 2.2a and 2.2b show mean temperature anomalies (the difference between the measured profile and the average of all measurements in that 1°x1° box over the entire month) during the convective stages in February 2003 and in July 2003. Horizontal bars show the 95% confidence interval for the mean of temperature anomalies. In agreement with expectations, the anomalies during stage 1 are small because convection has not yet fully started in this stage. Only small numbers of convective events are sufficiently intense, generating small anomalies in the

temperature profile. The anomalies grow progressively larger in stages two and three, as convection goes on progressively longer. In stage 4, the anomalies decrease as convection becomes weaker and begins to dissipate. For stage 5, after convection has terminated, the anomalies rapidly decrease to near zero. I also performed a diurnal separation: the over-plotted dotted line is from nighttime data only. AIRS measures the temperature profile twice a day, around 1:30am and 1:30pm in local time. There is no significant diurnal cycle in the anomalies. The implication of this lack of diurnal cycles will be discussed later.

We see that convection warms the troposphere up to an altitude of around 120 hPa, with cooling in the TTL between 120 and 70 hPa. The magnitude of the warming anomalies generally agrees well with previous studies. Sherwood and Wahrlich [1999] showed warming of up to 1.3 K, peaking around 300 hPa, during convection, using rawinsonde data from the Western Pacific area. Bhat et al. [2002] also demonstrated that, during the convective period, the atmosphere between 6 km and 13 km became warmer, and the amount of warming was less than 1.5 K relative to the mean temperature profile of the observation period.

Cold temperature anomalies at the tropopause level have also been seen previously in both observations [Johnson and Kriete, 1982; Sherwood et al., 2003] and in a model study [Kuang and Bretherton, 2004]. The amount of cooling in stage 3 is larger in February (~ -2.15 K) compared to that of July (~-1.87 K). Our result is larger than that of Sherwood et. al [2003], who found a cooling of ~1 K cooling just below the tropopause. Johnson and Kriete [1982] reported a rather large value, -6 K ~ -10 K,

studying three wintertime convections near Indonesia. I believe that this magnitude difference comes from the difference of sampling numbers, region and period. Kuang and Bretherton's [2004] model study also showed that a maximum cooling of ~10 K may be attributed to convective cooling at the cold point tropopause. Another minor discrepancy between this result and that of Sherwood and Wahrlich [1999] is that small local peaks of warm anomaly at the 150 hPa level exist in our study, which did not appear in Sherwood and Wahrlich [1999]'s analysis. In addition, I performed the same analysis with data over continents (Fig.2.3), which is invalidated by data quality assurance flags in the current version of retrieval, and found a similar temperature anomaly pattern with that over ocean. The only discrepancy was bigger anomalies near the surface, showing the effect of the smaller heat capacity of land.

2.3.2 Cooling rate calculation

Another quantity of interest is the tropopause cooling rate due to convection. To obtain this, I plot the elapsed time since convection started against the 100-hPa potential temperature anomaly (temperature anomalies at a pressure level P are converted to potential temperature anomalies by multiplying by $(P/P_o)^{-2/7}$, where P_o is 1000-hPa). The potential temperature anomalies as a function of time since convection started are shown in Fig 2.4. Symbols indicate convective stages. A least-squares fit to the data is shown as a dotted line, and its slope is the cooling rate. The estimated

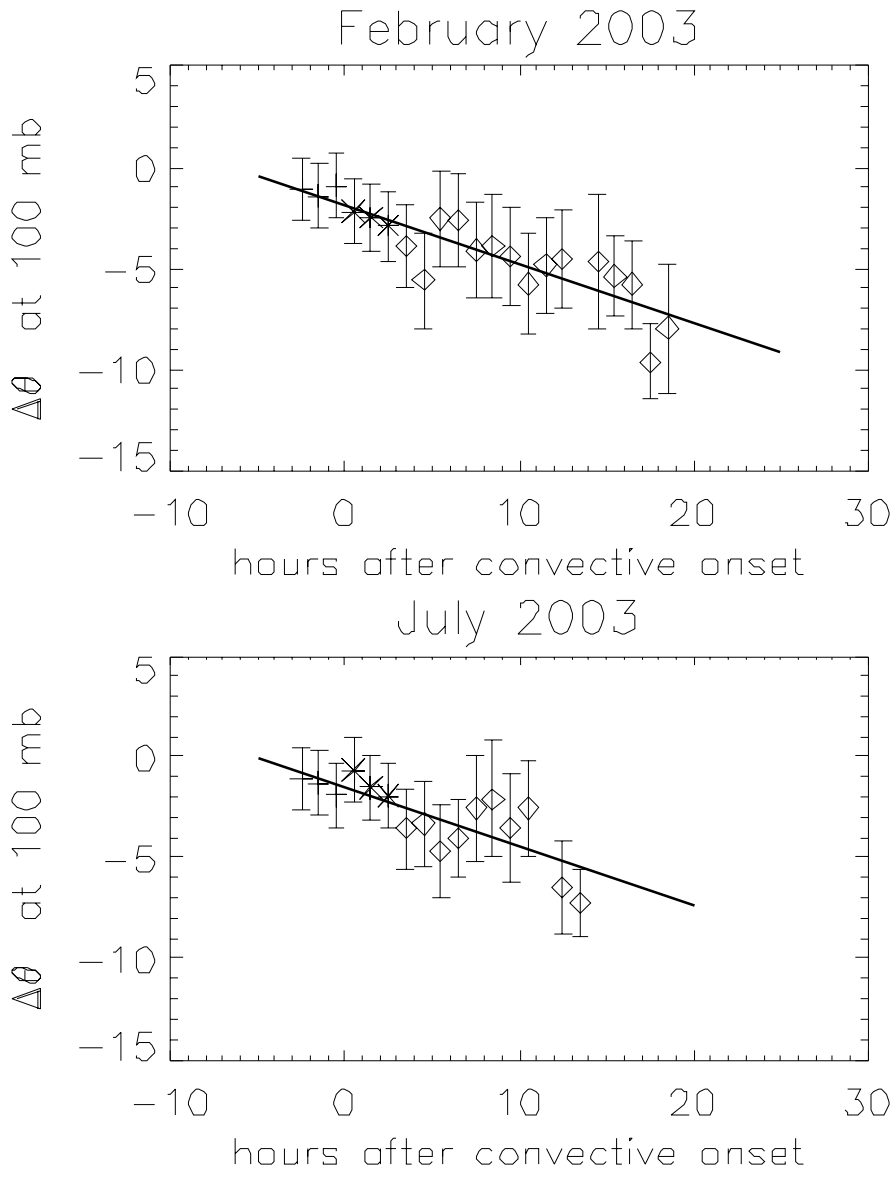

Figure 2.4 Cooling rate calculation for Feb. 2003 and for Jul. 2003. Shown symbols are the potential temperature anomaly at 100 hPa averaged in 1-hour bins of time after convection starts. Symbols +, * and diamond represent stage 1, 2, and 3. Estimated cooling rates are - 7 K/day in both months.

cooling rate (in potential temperature units) at the tropopause from this line fit is –7 K/day in both months. This cooling rate agrees well with the estimate by Sherwood et al. [2003], -5 ~ -10 K/day. Kuang and Bretherton [2004] also showed a cooling rate of a few tenth of a K/day in the tropical mean.

2.3.3 Sensitivity tests

There are two arbitrary thresholds used in this analysis, 208K, which is the threshold T_b representing "deep convection", and 10%, which is the fraction of pixels with brightness temperature less than T_b required before a region is considered to be "convective". I denote these terms as the T_b threshold (208 K) and the fractional threshold (10%), respectively. Figure 2.5 show how our results change when these two thresholds are adjusted. Figure 2.5a shows the average 100-hPa anomaly during stages 2 through 4 as a function of the fractional coverage of deep convection. The different symbols in the figure show the results for different values of T_b. As one might expect, using either a lower value of T_b or a higher required fraction of convective pixels results in larger (more negative) temperature anomalies. This makes sense because both of these represent more vigorous convection, which should also be associated with stronger cooling. Indeed, results show some dependency on the fractional threshold, while the dependency on the T_b threshold is not so strong. This result is consistent with that expected from Fig. 2.1, showing that the fractional threshold affects the convective stage determination more than the T_b threshold does. However,

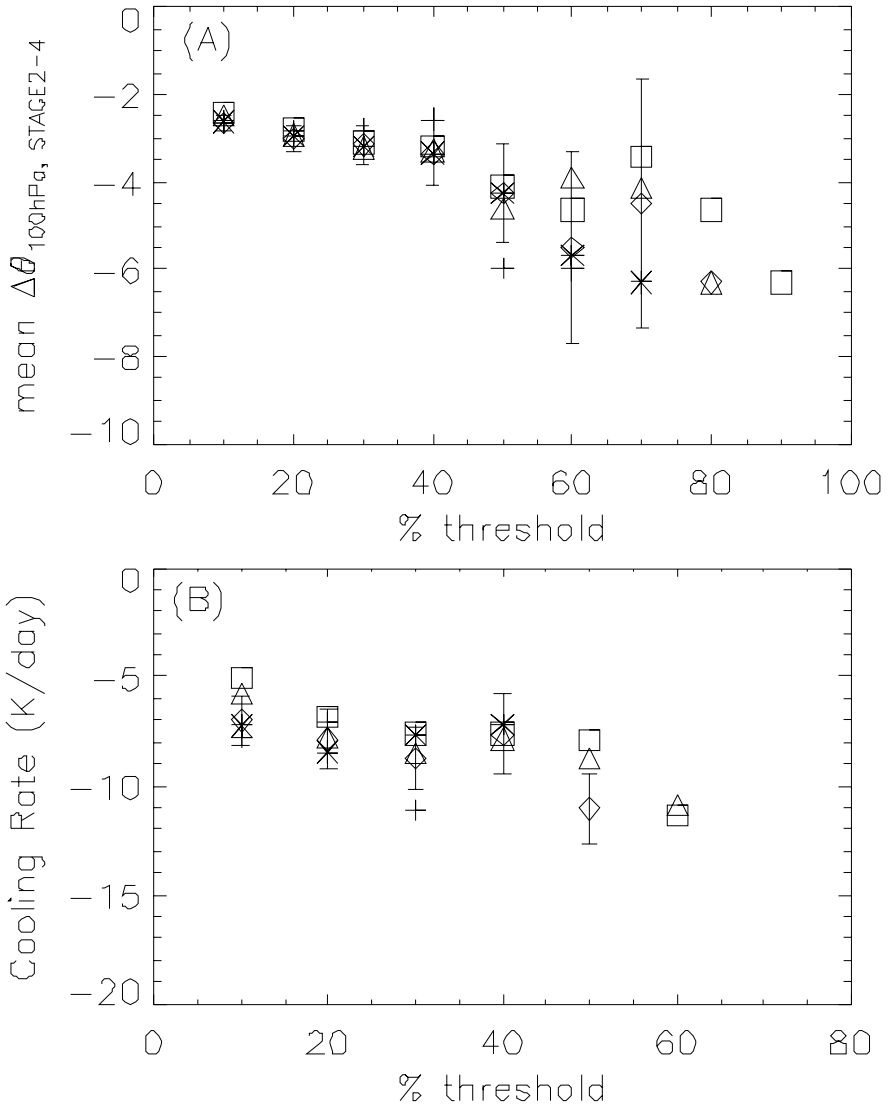

Figure 2.5 Sensitivity tests in (a) mean potential temperature anomalies at 100 hPa during convective event (stage 2-4), and (b) estimated cooling rates. Symbols indicate different "deep convection" thresholds. Changes in T_b threshold are shown as different symbols (Symbols +, *, ◊, □, and Δ indicate T_b threshold 204K, 206K, 208K, 210K, and 212 K, respectively), and the changes of fractional threshold are shown in x-axis. Error bars show the confidence intervals when 208K is used as the T_b threshold.

in overall, the sensitivity of the cooling amount to both thresholds is not significant, especially in the lower fractional threshold. For higher fractional thresholds, over 50%, the number of available cases decreases rapidly, so results are mostly scattered. This sensitivity test is consistent with Sherwood and Wahrlich [2003], who also showed that the results were not sensitive to the lower fractional threshold. The sensitivity test of the cooling rate also shows no significance, with values between -5 and -10 K/day in the lower fractional threshold range. This can be seen in Fig. 2.5b. A similar sensitivity test was performed by changing the box size to 2°x2°, and no significant difference was found.

2.3.4 Regional distribution

The regional distribution of the 100-hPa cooling during convective events (stages 2 through 4) is shown in Fig. 2.6. Significant tropopause cooling occurs in the southern Indian Ocean and central Pacific (February), and in the Asian Monsoon area (July). Superimposed solid lines are the percentage of deep convection – the fraction of pixels with brightness temperature below 208 K, measured by the Visible and Infrared Scanner (VIRS) [Kummerow et al., 1998] onboard the Tropical Rainfall Measuring Mission (TRMM) [Simpson et al., 1996]. Plotted lines are 1, 3, and 5 % levels. The brightness temperature of 208K is a typical temperature for the bottom of the TTL, so these contours indicate the locations of where clouds penetrate the TTL. The distribution of the tropopause cooling amount generally matches well with the

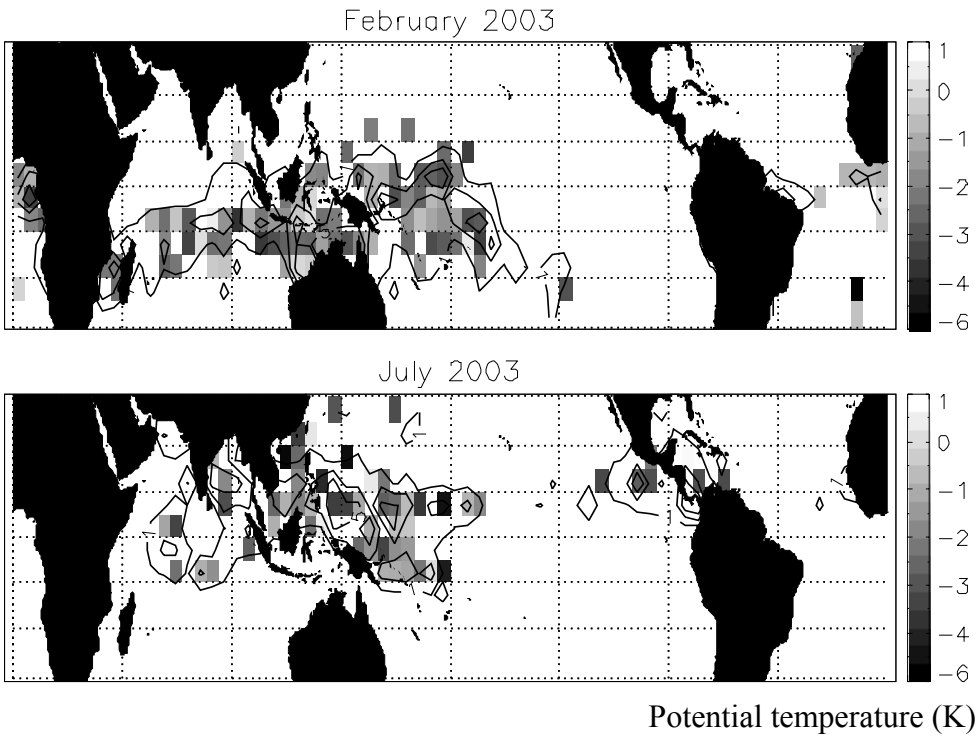

Figure 2.6 Regional distribution of the potential temperature anomaly at 100hPa during convective event (stage 2 through 4), averaged in 5x5 degree boxes. Superimposed lines are frequency of deep convection, the fraction of T_b below 208K measured by the VIRS. 1, 3 and 5 % lines are shown.

distribution of overshooting frequency, which provides a check that the convective cooling is somehow related to the occurrence of high cloud in the TTL.

2.4 Discussion

2.4.1 Cold point analysis

There are several previously identified mechanisms that can explain this convective cooling. This includes forced mesoscale ascent near the tropopause, which would lead to adiabatic cooling [Johnson and Kriete, 1982; Fritsch and Brown, 1982]. Using simple wave propagation model, Sherwood et al. [2003] demonstrated that the cold anomaly below 100-hPa can be partly accounted for by adiabatic lofting associated with wave propagation by heating in the troposphere, though cold anomaly succeeded in extending to the tropopause level only with strong heating cases. Sherwood et al. [2003] also argued that there is a diabatic component to the motion. They deduced this by assuming that the "cold point" of a profile was a material surface, and observing it has higher pressures and colder temperatures in response to convection. This result implies that the cold point's potential temperature decreased during convection, showing a diabatic processes. Our data does not have sufficient vertical resolution to verify or contradict this conclusion.

2.4.2 Cloud-top radiative cooling

If the cooling is diabatic, there are several possible explanations. Radiative cooling from high and optically thick clouds is one. Model calculations suggest that cooling rates from cloud tops can be as high as 10 K/day [Ackerman et al., 1988]. Using this value for an upper limit, a simple calculation shows that radiative cooling from thick clouds is unlikely to explain our observed cooling rate. AIRS measurements have a horizontal resolution of 50 km by 50 km, so cloud coverage of about 75% over this area is required for a thick cloud to produce the observed cooling rate of 7.5 K/day.

To see if this is reasonable, Fig. 2.7 shows the distribution of the brightness temperature within 25 km (radius) of each temperature profile categorized as stage 3. Assuming the brightness temperature is close to the actual cloud top temperature, the distribution of brightness temperature can represent the distribution of cloud top height. I also put corresponding pressure levels estimated from each brightness temperature using the mean temperature profile of the 1°x1° box in the right, and the accumulated cloud fractions, from the top to each pressure level, in the middle. Only 8 % of convection reaches or exceeds the 100-hPa level. This is far below the 75% necessary to account for the cooling.

More strong evidence, showing that the cloud is not responsible for this cooling, comes from the diurnal separation of temperature anomaly. Figure 2.2 shows that the nighttime-only convective cooling agrees closely with the 24-hour average convective cooling. Since absorption of solar radiation makes an important contribution to cloud top radiative heating during the day, one would expect day-night differences between

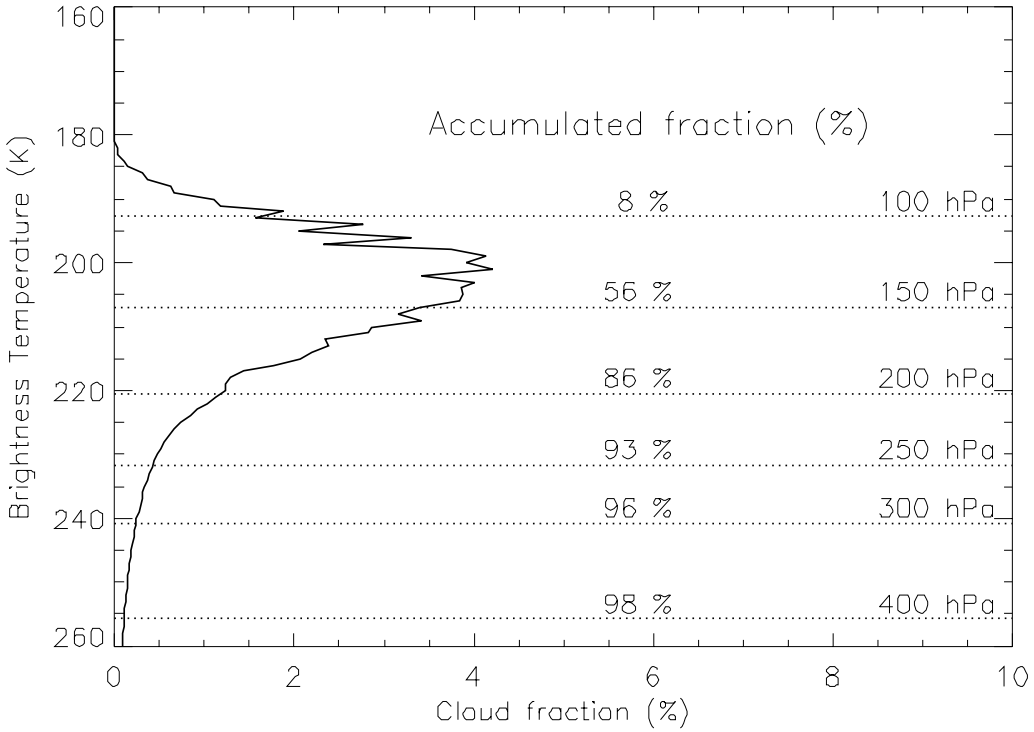

Figure 2.7 Distribution of cloud top heights in convective stage 3, estimated from the distribution of brightness temperature within 25 km (radius) of each temperature measurements. Accumulated cloud fractions, from the top to each pressure levels, are shown in the middle.

the daytime and nighttime convective cooling if clouds were responsible. We do not see that, suggesting that cloud top cooling from thick clouds is not the explanation.

Another explanation concerning the radiative effect is the radiative cooling from thin cirrus clouds that are located over thick cirrus clouds [Hartmann et al., 2001]. They used a simple radiative model to show that radiative cooling is produced by emission from thin cirrus ($\tau << 1$) at the tropopause if convective anvils with tops above 13 km exist below. The net cooling they estimate from this mechanism, however, is not more than 1 K/day, much smaller than the cooling rate measured in our study. In conclusion, this mechanism is not responsible for the observed convective cooling.

2.4.3 Mixing of overshooting clouds

The other explanation for diabatic tropopause cooling is the turbulent mixing of overshooting air with its environment [Sherwood, 2000]. Undiluted convection that rises above its LNB (i.e., is "overshooting"), will be colder than its environment. If this air subsequently mixes into the environment, it will cause cooling. A simple calculation demonstrates the potential of this process for cooling the TTL. Assuming mixing between air that ascends adiabatically to 100 hPa (with potential temperature θ_a) and environment (potential temperature θ), one can estimate how much overshooting air is needed to generate the cooling rate measured in Fig. 2.4. If mixing occurs, the temperature of the mixture will be determined by the ratio of the amount of

overshooting air and the amount of environmental air. Assuming the fraction of detraining air in the mixture is dr, the potential temperature of the mixture is

$$\theta_m = dr \cdot \theta_a + (1 - dr) \cdot \theta \tag{1}$$

The potential temperature difference between the mixture and the environment is

$$d\theta = \theta_m - \theta = \left(dr \cdot \theta_a + (1 - dr) \cdot \theta\right) - \theta \tag{2}$$

If we rearrange this equation for dr,

$$dr = \frac{d\theta}{\theta_a - \theta} = \frac{Q \cdot dt}{\theta_a - \theta} \tag{3}$$

where Q is the cooling rate, which we measured to be about –7 K/day.

For the usual values of potential temperatures (θ_a = 355 K at LNB and θ = 375 K at 100 hPa), the fraction of detraining air in the mixture that is needed to generate the -7 K/day cooling is

$$\frac{dr}{dt} = \frac{Q}{\theta_a - \theta} = \frac{-7K/day}{355K - 375K} = 0.35 \text{ (1/day)} \tag{4}$$

which implies approximately 35% of tropopause air should be replaced by overshooting convection in a day to satisfy the observed cooling rate. This is a difficult number to verify, but there are some estimates we can use. First of all, it should be noted that this turnover timescale is obtained only over a single convective event, not over the whole tropics. In our study, 3% of the total AIRS profiles were classified as 'convective' (stages 2 through 4), therefore, if we assume that all vertical mass transport from the LNB to the 100-hPa level occurs during these convections, the required fraction of air transported by overshooting to satisfy the observed cooling rate is 1.05 %/day (=35%/day × 3%), or a turnover time of approximately 3 months, in the tropical average. Dessler [2002] found a turnover time of 2 months near the tropopause, by analyzing ER-2 measurements of O_3 and CO. It looks reasonable that this amount is enough to cause the convective cooling rate observed in this study. Furthermore, in this calculation, I assumed the measured cooling is totally induced by turbulent mixing. If other processes can partly contribute to the measured cooling, the required overshooting amount will be lower, showing the turbulent mixing still has enough potential to cause convective cooling near the tropopause.

2.5 Conclusion

In this chapter, the effects of convection on the temperature structure of the TTL in February 2003 and July 2003 have been investigated using a global data set. This analysis indicates that a significant cold anomaly occurs in the TTL in response to

convection, in both day and night and during two times of year. The cooling rate is estimated to be around –7 K/day (potential temperature units) at 100 hPa during convection. While I cannot unambiguously assign a cause to this cooling, I do not believe it arises from radiation from either thick or thin clouds.

I do show that the mixing-in of cold air from overshooting convection is a potentially reasonable explanation for the cooling. This air detraining from overshooting deep convection is not only cold but also might be very dry, and so might also play an important role in determining the humidity level in the TTL and in the lower stratosphere.

Chapter 3. A study of tropical deep convective cloud mixing near the tropopause

3.1 Introduction

The question of how air is dehydrated as it enters the stratosphere is one of the classic problems of atmospheric science. Despite several decades of research, there are still important uncertainties concerning the mechanisms responsible for the stratosphere's extreme aridity [Gettelman et al., 2000]. This study focuses on a region called the tropical tropopause layer (TTL): a transition layer between the troposphere and the stratosphere, having properties of both. Processes occurring in the TTL define the stratospheric chemical boundary condition, especially the distribution of water vapor.

Air detraining from convection in the TTL subsequently experiences slow ascent as part of the mean overturning stratospheric circulation and rises toward the stratosphere. As the air slowly ascends, it is periodically exposed to temperatures considerably below that of the zonally averaged tropopause. These arise for a number of reasons, such as radiative cooling above deep convection [Hartmann et al., 2001] or

atmospheric waves [Potter and Holton, 1995; Boehm and Verlinde, 2000], to name just two. One theory of stratospheric dehydration postulates that formation and subsequent sedimentation of particles could occur during these episodic exposures to very cold temperatures, leading to dehydration [Holton and Gettelman, 2001]. The other theory postulates that air detrains from convection already dehydrated to stratospheric abundances [Sherwood and Dessler 2000; Sherwood and Dessler 2001]. In this case, no further dehydration is needed.

The convective dehydration theory [Sherwood and Dessler 2000; Sherwood and Dessler, 2001] requires overshooting deep convection to reach the tropopause and higher in order to expose the air to temperatures low enough to dry the air to stratospheric abundances [Johnston and Solomon, 1979]. Measurements show that the equivalent potential temperature (θ_e) in the boundary layer of convective regions peaks at 345 K and is generally less than ~355-360 K [Folkins et al., 2000]. Thus, convection reaching potential temperatures higher than ~355-360 K has likely overshot its level of neutral buoyancy (LNB). We call this 'overshooting' deep convection. If this air subsequently mixes with higher potential temperature air during the time it is above its LNB, then the resulting mixture will settle at altitudes above the parcel's initial LNB. In the absence of mixing, the convecting air will eventually reach equilibrium at its LNB.

Evidence that clouds penetrate to near the tropopause is based largely on field missions that provide results for a single time and place [Cornford and Spavins, 1973; Danielsen, 1993; Kritz et al., 1993]. Observations of clouds during these missions do

not quantitatively indicate the extent to which they are mixing with their environment. Global analyses of cloud height do exist [e.g., Gettelman et al., 2002]. These analyses usually use brightness temperature from satellites to infer cloud height. However, the conversion from brightness temperature to altitude is uncertain [Sherwood et al., 2004] and therefore conclusions reached from these analyses require independent verification. In this study, an alternative method is used to determine the height of convecting clouds, as well as how much they mix with air in the TTL.

3.2 Data

To study overshooting convection, the data from the Visible and Infrared Scanner (VIRS) [Kummerow et al., 1998] onboard the Tropical Rainfall Measuring Mission (TRMM) [Simpson et al., 1996] are utilized. Four time periods (January 1998, July 1998, January 1999, and July 1999) are used in the analysis. These years are characterized by winter and summer seasons from both an El Nino (1998) and La Nina year (1999). VIRS makes measurements at five wavelengths (0.63-, 1.6-, 3.75-, 10.8-, and 12.0- μm) with a horizontal resolution of 2 km at nadir. In this study, data from the 0.63-, 3.75-, and 10.8-μm channels are used. In addition, the 2.5º × 2.5º surface temperature and relative humidity from National Center for Environmental Prediction (NCEP) reanalysis [Kalnay et al., 1996] are used as initial conditions of an adiabatic altitude model.

3.3 Methodology

Figure 3.1 shows a schematic picture of this study. It shows a cartoon of deep convective cumulonimbus, overshooting its LNB. After reaching its maximum height (Ht), the overshot cloud falls back and forms an anvil around its LNB.

Given appropriate sun angles, an overshooting cloud will cast a shadow on the surrounding anvil that can be seen in the VIRS visible and near-IR channels. Given the length of the shadow of an overshooting cloud, its height above the anvil can be calculated by simple geometry. As shown in Fig. 3.2a, dH, the height of the overshooting cloud above the cirrus anvil, is $L \cdot \tan(90-\theta)$ where L is the length of the shadow and θ is the solar zenith angle. It should be noted that this 'height' is the vertical distance between the cloud top and the anvil at the end of the shadow.

VIRS' 0.63- and 3.75-μm channels are visible and near infrared, respectively, so they primarily measure reflected solar radiation. These wavelengths can therefore be used to identify the far end of the shadow. The 10.8-μm channel, which measures emitted infrared radiation, is used to identify the highest point of the overshooting cloud, which is also the beginning of the shadow.

Figures 3.2b & 3.2c are examples of the shadow method. They are slices of TRMM data taken in the plane defined by the local vertical and solar zenith vector. Negative distances indicate the side of the overshoot facing the sun while positive distances indicate the other side. Figure 3.2b shows the 10.8-μm brightness temperature. There is a clear minimum in the data, which corresponds to the highest point of the overshooting convective cloud. Because this channel is mainly emissive,

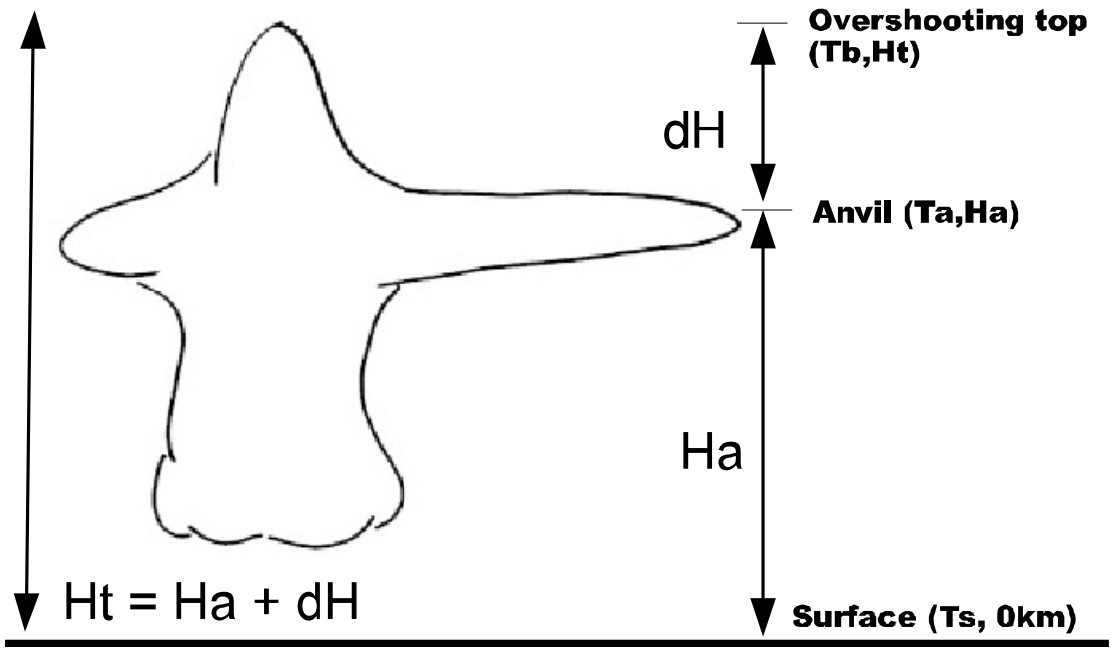

Figure 3.1 A cartoon of overshooting deep convective cloud. Vigorous cumulonimbus tends to overshoot to past the level of neutral buoyancy, then flows out to form an anvil outside. The total height of overshooting cloud top (Ht) is the sum of the anvil height (Ha) and the overshooting height (dH).

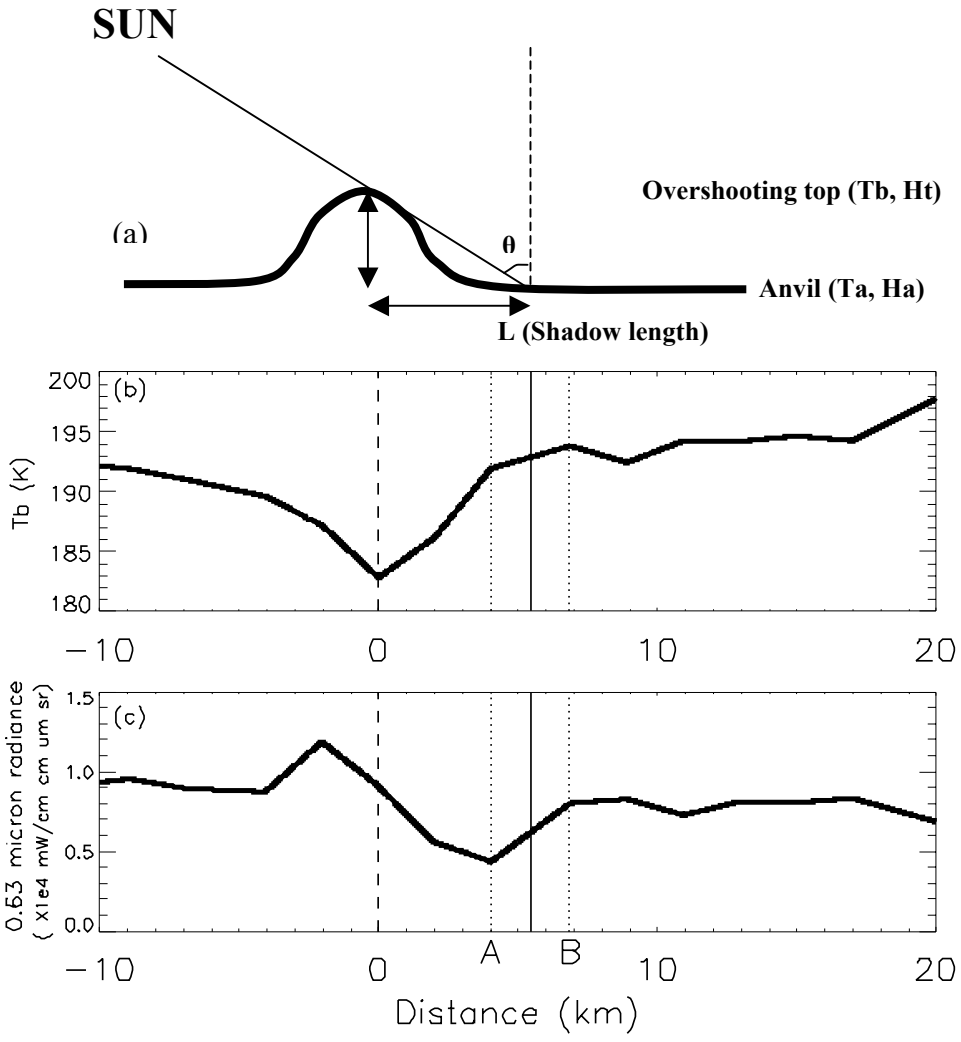

Figure 3.2 Concept of the cloud shadow method. (a) Overshooting cloud and the shadow it casts, (b) Infrared channel (10.8 μm) showing the location of the overshooting cloud, (c) visible channel (0.63 μm) shows the shadow. This overshooting event was measured at 24.5°E, 17.8°S on Jan. 20, 1998. Shadow edge is located at 5.45 km from the center of overshooting, and solar zenith angle is 69.6°. In this case, calculated overshooting height is 2.87 km. Lines labeled A and B are discussed in the text

there is, as expected, a general symmetry about the overshoot. Fig. 3.2c shows the 0.63-μm data, which is mainly reflected solar radiation. The amount reflected increases on the sun side of the overshoot and suddenly decreases after the overshoot. This pronounced decrease in signal on the side of the overshoot opposite from the sun is the shadow that the overshoot has cast on the surrounding cloud. Note that the enhanced radiance on the sun side has been attributed by Van Hees and Lelieveld [2000] to the change of the slope of reflecting surface. Structured cloud tops change the slope of illuminated cloud top surface, so they make more radiation to be reflected upward. 3.75-μm channel data are also used to identify the same phenomena.

Due to the ethereal nature of clouds and relatively coarse resolution of the VIRS data, it is impossible to define the exact position of the end of the shadow. In this study, the following recipe was used to determine the end of the shadow. Point A in Fig. 3.2c is the location of the minimum value of 0.63-μm radiance. The shadow end is assumed midway between this pixel and the adjacent pixel (denoted as B). Based on the length of the shadow and the solar zenith angle, the overshoot height dH is calculated.

3.4 The overshooting height calculation and analysis

3.4.1 The overshooting height calculation

We take TRMM data for an entire month and isolate those scenes that include 10.8-μm channel brightness temperatures below 200 K, which are typical anvil

temperatures, and solar zenith angles (SZA) between 50 and 80 deg. Higher and lower solar zenith angle cases were not used because the shadows they cast were too long or short for our algorithm. In the end, 762 cases (229, 167, 207, and 159 for Jan. 98, Jul. 98, Jan. 99, and Jul. 99, respectively) were identified from four one-month periods. The distribution of overshooting events is shown in Fig. 3.3.

Fig. 3.4 shows scatter plots of overshooting height above the anvil, dH, versus the difference between the temperature of the overshooting top (lowest brightness temperature) and the temperature of the anvil (at the tip of the shadow) for the four different months we investigated. The solid line is the adiabat, about 9.8 K/km. At the altitude of the tropical tropopause (~16km), water vapor mixing ratio is so low that there is little difference between the dry adiabat and the moist adiabat. This adiabat well reproduces the lower limit of the scatter plots, as one expected. This strongly suggests that our method is working as we expected.

Figure 3.5 shows the averages of all points from 4 months being investigated according to their minimum brightness temperature. Each point is a mean of all events whose minimum 10.8-μm channel temperature falls within a 5-K bin. This figure shows that the temperature difference between the overshooting cloud and the anvil is ~4 K km^{-1}, less than that predicted by the adiabatic lapse rate and also smaller than previously reported values of 9 K km^{-1} [Adler et al., 1983] or 8 K km^{-1} [Negri, 1982]. Obviously, some diabatic process must be occurring, which will be discussed later.

Note also that on average the coldest overshooting events (points 1 & 2 in Fig. 3.5) fall closer to the adiabat than warmer events. It seems likely that these very cold

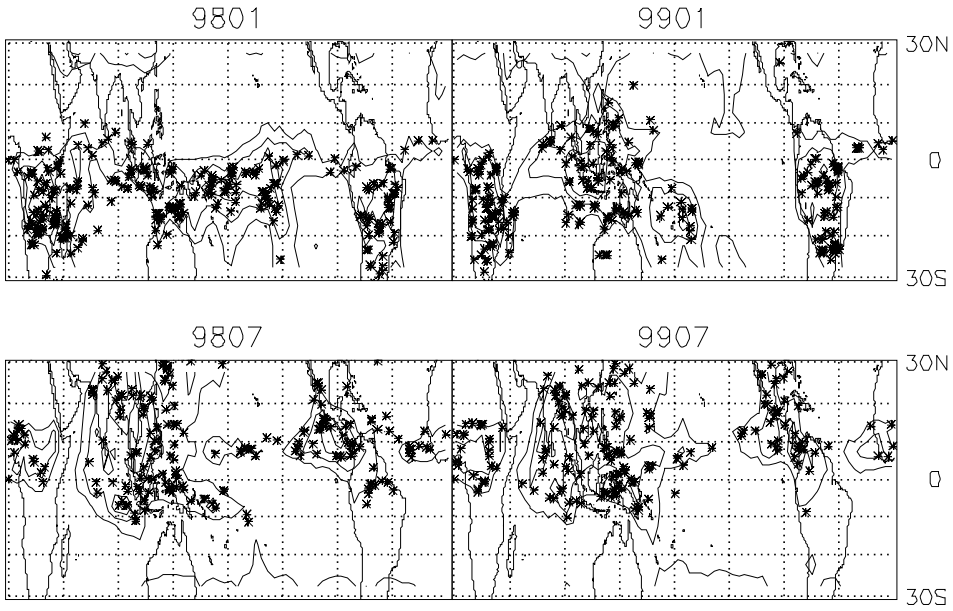

Figure 3.3 Geophysical distribution of overshooting events used in the analysis. Contours indicate monthly mean of 11-μm brightness temperature measured from VIRS. 260K, 270K, and 280K lines are shown.

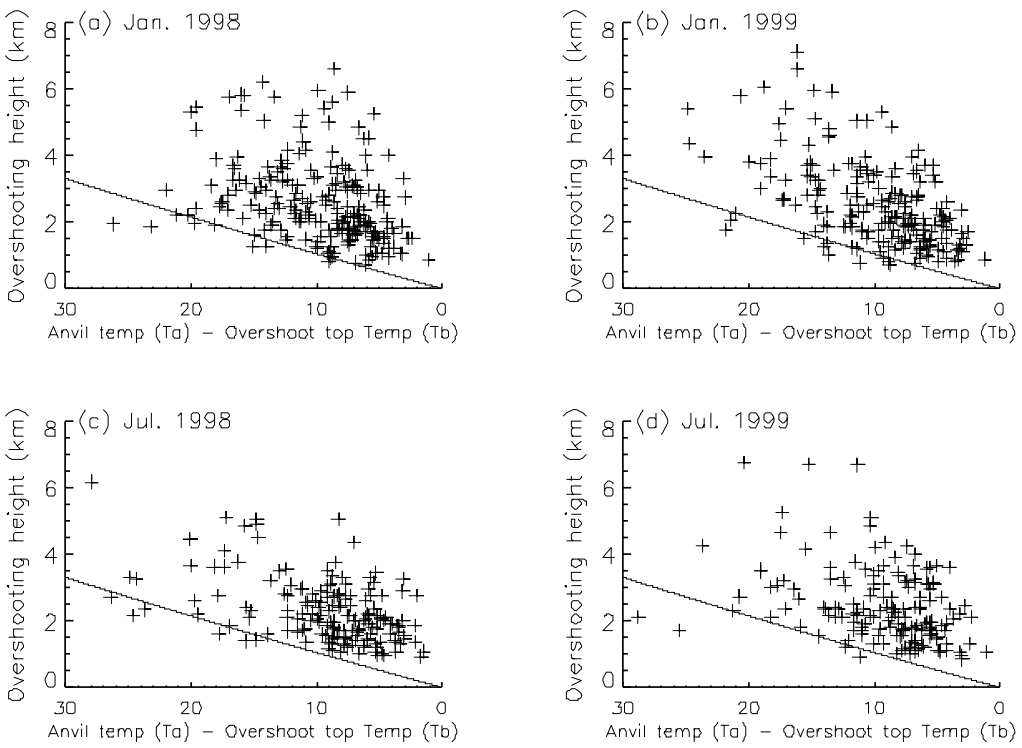

Figure 3.4 Scatter plots of overshooting height above the anvil (dH) and the difference between the temperature of the overshooting top and the temperature at the end of the shadow. The solid line is the moist adiabat.

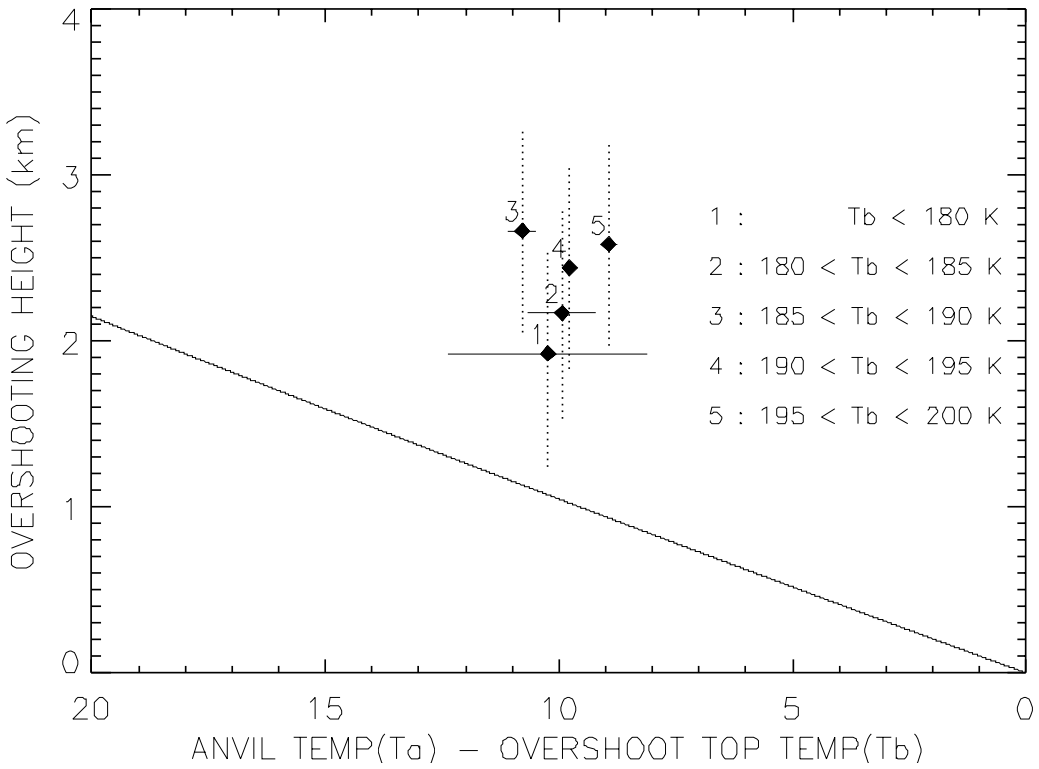

Figure 3. 5 Mean of scatter plots in Fig. 3.4 according to their minimum brightness temperatures. Tagged numbers indicate the temperature ranges used for each average. Solid line is the adiabat.

events are much more closely approximating an undiluted adiabatic trajectory than the warmer parcels. This makes sense: there is no way for a parcel to ascend from the surface via an adiabat, mix with the environment to any significant extent, and maintain a temperature below ~180 K.

3.4.2 Error analysis

There are three sources of error in the calculation of overshooting height. First, the resolution of a single measurement of the VIRS instrument is 2-3 km, thus one cannot place either the overshoot location (the beginning of the shadow) or the end of the shadow to better than this. If a shadow has a 2-km possible error in both ends (i.e. overshoot center and shadow end position), the total error in the length of the shadow is $2\sqrt{2}$ km (i.e. root-mean-square, RMS). Because the errors from different events are expected to be uncorrelated, the vertical error bars on each point in Fig. 3.5 are the RMS sum of the errors for the individual points divided by the square root of the number of points.

Second, the finite resolution of the data introduces a similar uncertainty in temperature. As one cannot place the exact beginning and end of the shadow, we cannot know their exact temperatures. As shown in Fig. 3.2b, the real anvil temperature is between the temperature at point A and the temperature at point B. The mean of both temperatures is taken as the anvil temperature and the temperatures of A and B are used as the limits of error. In most cases, they are less than 2-3 K. The

horizontal error bars in Fig. 3.5 are calculated from the propagation of these errors in the same way discussed above.

Third, an uncertainty arises because clouds are not solid bodies, and the different wavelengths "see" slightly different clouds because the cloud attenuates radiation of various wavelengths differently [Hunt, 1973]. To estimate the magnitude of this uncertainty on our estimation of the overshooting height, a simple sensitivity test was performed.

Figure 3.6 is a schematic of this problem. The 10.8-μm channel measures the temperature at one optical depth. The shadow, on the other hand, is determined by height at which the solar slant path at 0.63 μm is one optical depth. In the case shown in Fig. 3.6, the 10.8-μm channel reads the temperature at h_{IR}, but the shadow length is defined by a cloud of height h_{VIS}. Thus, in calculating the lapse rate, there is a mismatch between the temperature difference and the height. One can consider this an error in either the length of the shadow or in the temperature of the overshoot - which one we choose is arbitrary. I will ascribe the error to the length of the shadow.

A simple calculation will help quantify this error. First, assuming values for the effective radius and ice water content, the distances corresponding to one optical depth in both channels is estimated [Fu and Liou, 1993]. One further assumes that the cloud's shape can be described by a Gaussian distribution ($A*\exp(-x^2/(2s^2))$), with its height and width defined by the parameters A and s. Assuming a homogeneous extinction coefficient (i.e. constant particle size and ice water content) [Ou et al., 1993], one can estimate the height difference caused by the error in the shadow length. For

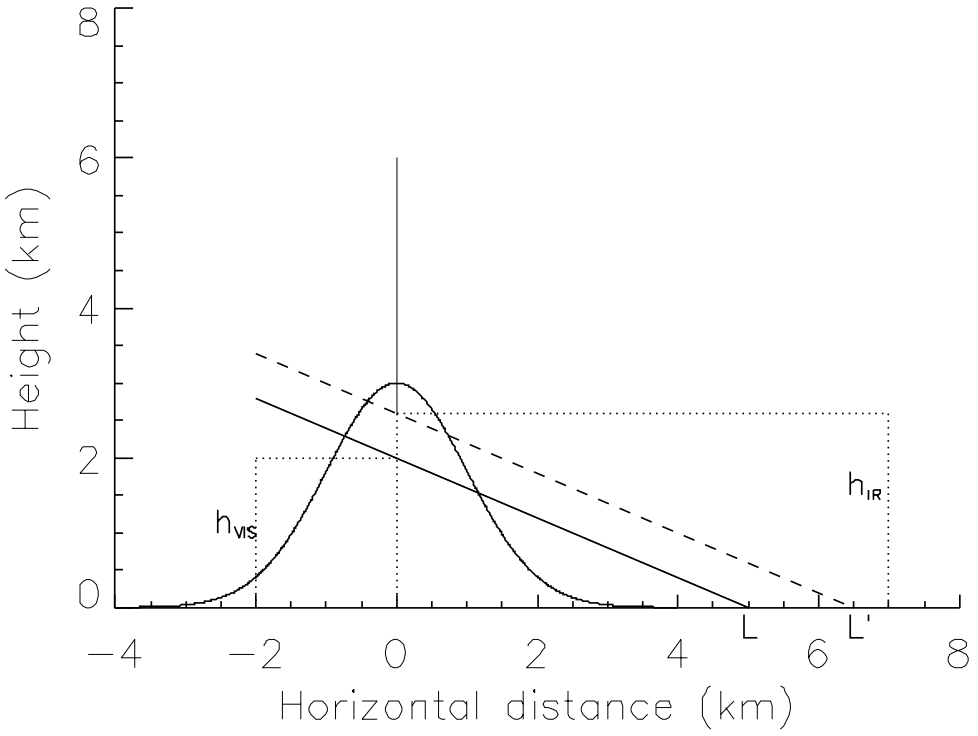

Figure 3. 6 A schematic of possible errors due to different optical depths of 10.8-μm and 0.63- μm. The 10.8-μm channel measures the temperature at h_{IR} after penetrating one optical depth. The height we measured from the shadow length is h_{VIS} if L is measured shadow end.

example, if we use A = 3 km, s = 1, θ = 70°, De = 34μm, and IWC = 0.03 g/m^3 (where θ, De, IWC represent solar zenith angle, effective diameter of cloud particle, and ice water content, respectively), the overestimated height ($h_{VIS} - h_{IR}$) is 0.29 km. On the other hand, with A = 3 km, s = 0.5, SZA = 69°, De = 31μm, and IWC = 0.03 g/m^3, the difference is 0.20 km ($h_{IR} > h_{VIS}$). Calculations for 1 km < A < 6 km, 0.5 < s < 2, 50° < θ < 80°, 1 < De < 100 μm, and 0.01 g/m^3 < IWC < 5 g/m^3 were performed [Rosenfeld and Lensky, 1998; Sherwood, 2002], and results show that, for the most of cases, the difference in inferred heights are within ± 0.6 km. Even for larger particle sizes and smaller ice water content, which results in longer paths through the cloud, the difference remains generally small. This error is also reflected in the vertical error bars in Figs. 3.5. Thus, the vertical error bars are the RMS of the error due to the resolution limit and the error due to different optical depths discussed here.

3.4.3 Implication to the humidity regulation in the TTL and lower stratosphere

Consequently, the difference between the inferred lapse rates on the overshoots and the adiabat in Fig. 3.5 cannot be explained by errors in the calculation. This conclusion is an intriguing result. The most likely explanation is the mixing of air in the overshooting convective cloud with the warmer environment. This mixing increases the parcels' temperature and potential temperature, and hence its LNB, allowing the air to reach equilibrium within the TTL. This is consistent with recent

work by Dessler [2002], who used O_3 and CO as tracers of convection to show that significant detrainment was occurring near the tropopause, at potential temperatures well above those found in the boundary layer.

3.5 Total height calculation

In the previous section, the overshooting heights of convective clouds were estimated. If we also estimate the height of the anvil, it is possible to estimate the total height, which is the sum of the anvil height and the overshooting height. A simple adiabatic calculation can help estimate the height of the anvil. The temperature at 14 km, the base of the TTL, is very close to that predicted by a moist adiabat rising from the surface. This is consistent with the fact that 14 km is approximately the upper limit of the LNB for deep convection. Thus, for altitudes near 14 km, we can use an adiabatic temperature profile to convert temperature to altitude.

To perform this calculation, two sources of error should be considered. First, this adiabatic temperature-altitude conversion is a little sensitive to the change of the surface temperature and the relative humidity (Fig. 3.8). Combined with the individual overshooting height errors discussed above, it can cause an error of 3-4 km in the total height calculation in our analysis. Second, because it is doubtful that the temperature at any level above 14 km could be colder than an adiabat, using the adiabatic altitude calculation provides a lower limit of the altitude, which implies a potential low bias in height. Figure 3.8 shows the total height calculated using the 2.5° × 2.5° NCEP

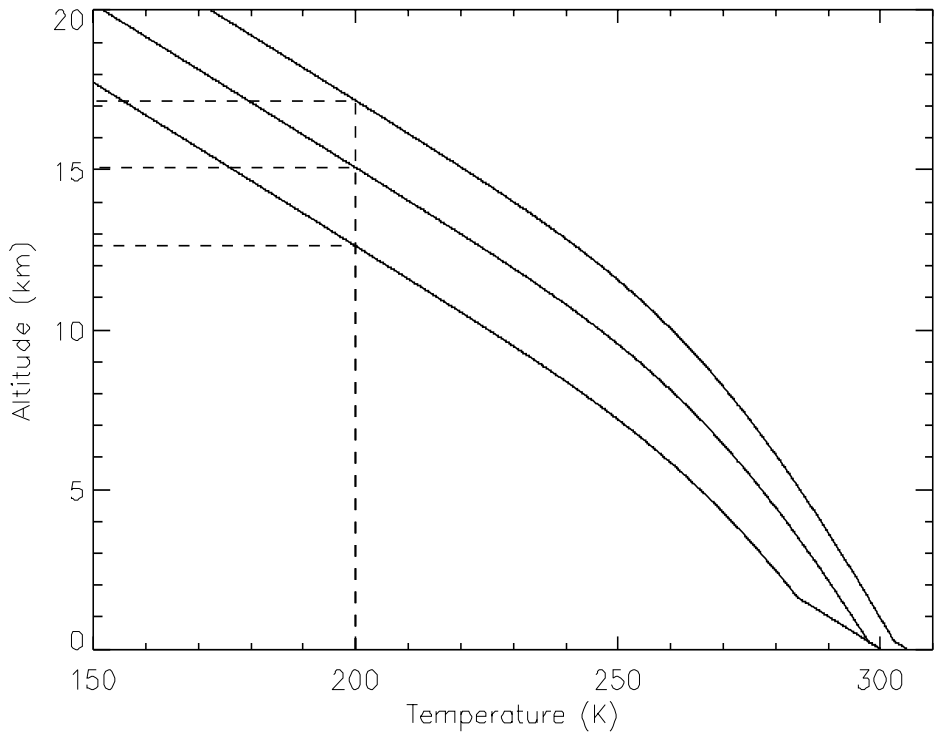

Figure 3. 7 A moist adiabatic model to convert temperature to altitude. Estimated altitude is a function of surface temperature and surface relative humidity. Three lines show moist adiabat with different surface conditions: T_s = 305K, f = 80 % (upper line), Ts = 300K, f = 80 % (middle line), and T_s = 300K, f = 50 % (lower line).

reanalysis surface temperature and relative humidity [Kalnay et al., 1996], interpolated to the specific overshoot locations, as initial conditions for the adiabatic altitude calculation. In spite of the large ambiguity mentioned above, it is very obvious that there exist overshoots reaching high enough throughout the TTL. Figure 3.8 also confirms the result discussed in the section 3.4.1 - the overshoots are warmer than an adiabatic calculation would predict. This is consistent with the idea that some mixing is occurring between these clouds and the TTL environment.

3.6 Conclusions

In this chapter, I have calculated the heights of overshooting cloud tops from the size of the shadows they cast. The existence of high overshoots is important in understanding the physics of the TTL and has important implications for the dehydration mechanism of the stratosphere. I measure overshoots going well above typical tropopause altitudes — about 16.5 km.

These overshoots are warmer than predicted by undiluted adiabatic ascent from the surface. This suggests that the brightness temperature alone will underestimate the height of the clouds. Mixing of air with its environment is a possible explanation for the departure from the adiabatic lapse rate. Because of this mixing, this air will reach equilibrium at an altitude above the LNB predicted by boundary layer θ_e.

I have shown in this paper that convection clearly extends throughout the TTL and that the overshooting clouds are mixing with the TTL air. This is in agreement

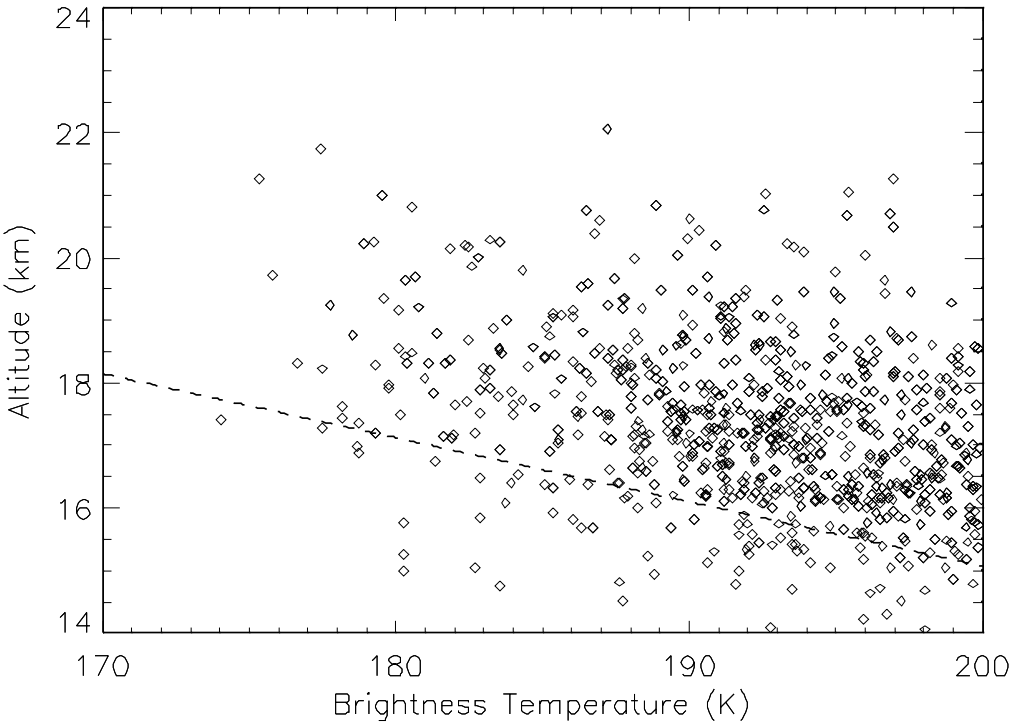

Figure 3. 8 Total heights of the overshooting convective clouds estimated by adding the overshooting height and the anvil height. Dashed line indicates the moist adiabat with T_s = 300 K, P_s = 1013.25mb and rh = 0.8.

with previous work [e.g., Sherwood and Dessler, 2001; Dessler, 2002] and is a potentially important process occurring in the TTL.

Chapter 4. Summary and Conclusions

The question of how temperature is regulated in the transition region between the tropical troposphere and the stratosphere is of great interest because this region's temperature plays an important role in controlling the lower stratospheric humidity. This transition layer, referred to as the Tropical Tropopause Layer (TTL), is defined as lying between the zero net radiative heating level and the highest level that convection reaches. This dissertation focuses on the role of overshooting deep convection in the regulation of temperatures in the TTL.

This dissertation includes two important conclusions concerning temperature regulation in the TTL. First, significant cooling near the tropical tropopause is observed during the time when active convection is occurring. Mixing-in of detrained air from overshooting deep convection likely plays an important role in this cooling. Second, there exist overshooting deep convections that penetrate several kilometers over the level of neutral buoyancy. Analyzing the thermal structure in these clouds reveals that the estimated lapse rate in the overshooting deep convection is far below the adiabatic lapse rate, implying that significant mixing occurs between overshooting clouds and environmental air.

4.1 Observation of convective cooling in the TTL

Chapter 2 shows how temperature profiles are affected by the progression of local convection. In order to observe the effect of deep convection on the thermal structure of the TTL, a composite technique is used to relate the local temperature anomalies to the evolution of local convection. Two data sets are used in the analysis. First, the local temperature anomaly is determined from temperature profiles measured by the Atmospheric Infrared Sounder (AIRS) onboard the *Aqua* satellite. Second, the time evolution of local convection is determined by the National Centers for Environmental Protection / Aviation Weather Center (NCEP/AWS) half-hourly infrared global geostationary composite.

The results of this analysis show that there are cold temperature anomalies near the surface and warm temperature anomalies in the middle troposphere, in response to active convection. The results also show that the TTL is cooled by convection, in agreement with previous observations and model simulations. By using a global data set, the variations in this convective cooling were investigated by season and region. There are no significant differences between the results from February 2003 and July 2003. The regional distribution of convective cooling generally matches well with the distribution of the frequency of overshooting convection, implying that convective cooling is related to the occurrence of high clouds in the TTL.

In order to see how fast this convective cooling occurs, the cooling rate is estimated for each month. Data from both seasons show significant cooling rates, around -7 K/day. There are several possible explanations for this convective cooling, which include adiabatic lifting by meso-scale ascending motion or wave propagation, cloud-top radiative cooling, and turbulent mixing of overshooting clouds. Several analyses have been performed to check the possible explanations, with the following results:

• This study could not clearly separate how much of the observed convective cooling is adiabatic and how much of it is diabatic. Previous research has shown that adiabatic lifting has partly contributed to this tropopause cooling, but cold point analysis by Sherwood et al. [2003] demonstrated that the observed cooling is induced by diabatic processes.

• Diabatic tropopause cooling can be caused by radiative effects at the tops of clouds, which includes radiative cooling at the top of high and optically thick clouds, and radiative cooling by thin cirrus clouds with deep convection lying below. In both cases, I strongly conclude that radiative effects are not the explanation for the observed convective cooling. First, the number of clouds reaching the tropopause level is not enough to explain the observed cooling. Second, the observed cooling shows no difference in the diurnal separation. Because absorption of solar radiation makes an important contribution to cloud-top radiative heating during the day, one would expect

a significant difference occurs between analyses from day-time and night-time data. However, there is no diurnal difference in the amount of convective cooling, showing that cloud-top radiative effects are not responsible for the observed convective cooling.

- The most likely explanation for this convective cooling is turbulent mixing of overshooting clouds. While only a small fraction of convection extends to near the tropical tropopause, I have performed a calculation that shows infrequent overshooting still has potential to cool the tropopause effectively.

4.2 Overshooting cloud height calculation

Chapter 3 focuses on features of overshooting deep convective clouds. Though overshooting deep convective clouds may work to cool the tropical tropopause, it is still unclear how high these clouds can reach, and if there is sufficient mixing between these clouds and the environmental air.

Most research on the height of convective clouds relies on the measurement of thermal brightness temperatures. Cloud-top height for a deep convective cloud is obtained by observing its brightness temperature and matching this to a local temperature sounding. Since this method contains some inevitable uncertainties, this study uses an alternative method: the height of an overshooting convective cloud is estimated from the length of the cloud's shadow. Given appropriate sun angles, an overshooting cloud will cast a shadow on the surround anvil. The length of the shadow

is estimated from visible and near-infrared channels of the Visible and Infrared Scanner (VIRS) onboard the Tropical Rainfall Measuring Mission (TRMM) satellite, and the height of the cloud is estimated through simple geometry.

762 cases from 4 months are analyzed. The results show a cloud can overshoot several kilometers above its anvil, which usually forms at or slightly above the level of neutral buoyancy. I also performed a calculation to estimate the lapse rate in the cloud: approximately 4 K/km.

This result clearly shows that the measured lapse rate of these clouds is significantly below the adiabatic lapse rate. Considering an undiluted overshooting cloud follows the adiabatic process, this result implies a significant amount of diabatic processes occur. I suggest that mixing between these clouds and the near-tropopause environment could be an explanation for the diabatic warming in the overshooting clouds. As a result, these clouds will likely settle at a final altitude above the convections' initial level of neutral buoyancy. If this mixing occurs, overshooting clouds can play an important role in the transport of tropospheric air deep into the TTL.

Total heights of overshooting deep convective clouds were also estimated based on the overshooting height estimated by the shadow method and the anvil height estimated from the moist adiabat model. In spite of possible errors in this estimation, it is obvious that there exist overshooting clouds reaching throughout the TTL.

4.3 Overshooting deep convection and dehydration in the lower stratospheric humidity

The findings in this dissertation have important implications for explaining the mechanism of tropical lower stratospheric humidity regulation. Since Brewer postulated the Brewer-Dobson circulation, the question of how air is dehydrated as it enters the stratosphere is one of the classic problems of atmospheric science. Processes in the TTL are important because they control the humidity of air entering into the tropical lower stratosphere.

There are several theories that postulate how air enters the lower stratosphere and how this air is dehydrated to the level of lower stratospheric humidity. Air detraining from convection in the TTL subsequently experiences slow ascent as part of the mean overturning circulation and rises toward the stratosphere. As the air slowly ascends, it is periodically exposed to temperatures considerably below that of the zonally averaged tropopause. One theory postulates the formation and subsequent sedimentation of particles could occur during these episodic exposures to very cold temperatures, leading to dehydration. The other theory postulates that air detrains from overshooting deep convection already dehydrated to stratospheric abundance. The convective dehydration theory requires overshooting deep convection to reach the tropopause and higher in order to expose the air to temperatures low enough to dehydrate the air to stratospheric humidity levels.

This dissertation reveals important points about the convective dehydration theory. First, this study demonstrates that the TTL is cooled by convection, at a rate of

–7 K/day. This cooling speed is beyond the range that is explained by radiative cooling at the top of convective clouds, and mixing of detrained air from deep convection into the TTL air is a likely explanation for this convective cooling. One problem with this hypothesis of convective cooling by the mixing of overshooting clouds is whether there occurs enough overshooting deep convection to contribute sufficient cooling in the TTL. In general, it is agreed that only a small fraction of convection extends to the vicinity of the tropical tropopause. However, this study shows that infrequent events still have an effect in cooling the TTL.

Second, another necessary condition for this convective dehydration theory is that deep convection overshoots high enough over its level of neutral buoyancy, and that it mixes into the lower stratospheric air to remain in the higher level. Analysis using the TRMM VIRS data shows that there exist overshooting deep convections that penetrate into the lower stratosphere, and these clouds reach several kilometers over their anvils, throughout the TTL. Analysis on the thermal structure in the overshooting cloud also shows that the lapse rates in these clouds are around 4K/km, which is far below the adiabatic lapse rate, 10 K/km, near the tropical tropopause. The only way to maintain this lapse rate is by mixing of overshooting air into the environment. Air detrained from overshooting deep convective clouds is not only very cold but also very dry, if efficient sedimentation occurs during the time of ascending. Thus, it has an important role in explaining the dehydration in the tropical lower stratosphere.

The mechanisms of dehydration in the tropical lower stratosphere is an important scientific topic that has been debated for a long time. It seems there is no simple

answer, and phenomena from various scales, from micro-scale process in the clouds to the large-scale circulation, are involved together. This dissertation provides evidence that overshooting deep convection plays an important role in the process of the regulation of tropical lower stratospheric humidity.

References

Abbas, M. M., H. A. Michelsen, M. R. Gunson, M. C. Abrams, M. J. Newchurch, R. J. Salawitch, A. Y. Chang, A. Goldman, F. W. Irion, G. L. Manney, E. J. Moyer, R. Nagaraju, C. P. Rinsland, G. P. Stiller, and R. Zander, Seasonal variations of water vapor in the lower stratosphere inferred from ATMOS/ATLAS-3 measurements of H_2O and CH_4 , *Geophys.Res.Lett.*, **23**, 2401-2404, 1996.

Ackerman, T. P., K. N. Liou, F. P. J. Valeroj, and L. Pfister, Heating rates in Tropical Anvils, *J.Atmos.Sci.*, **45**(10), 1606-1623, 1988.

Adler, R. F. and R. A. Mack, Thunderstorm Cloud Top Dynamics as Inferred from Satellite Observations and a Cloud top Parcel Model, *J.Atmos.Sci.*, **43**, 1945-1960, 1986.

Adler, R. F., M. J. Markus, D. D. Fenn, G. Szejwzch, and W. E. Shenk, Thunderstorm top structure observed by aircraft overflights with an infrared radiometer, *J.Climate Appl.Meteor.*, **22**, 579-593, 1983.

Alexander, M. J. and L.Pfister, Gravity wave momentum flux in the lowerstratosphere over convection, *Geophy. Res. Lett*., **22**(15), 2029-2032,1995

Atticks, M. G. and G. D. Robinson, Some features of the structure of the tropical tropopause, *Q. J. R. Meteorolo. Soc*., **109**(460), 295-308, 1983

Bhat, G. S., A. Chakraborty, R. S. Nanjundiah, and J. Srinivasan, Vertical thermal structure of the atmosphere during active and weak phases of convection over the north Bay of Bengal: Observation and model results, *Curr. Sci. India.*, **83** (3), 296-302, 2002.

Bignell, K., The water vapour infrared continuum, *Q. J. R. Meteorolo. Soc*., **96**, 390-403,1970

Boehm, M. T. and J. Verlinde, Stratospheric influence on upper tropospheric tropical cirrus, *Geophys.Res.Lett.*, **27**(19), 3209-3212, 2000.

Brasseur, G. P. and S. Solomon, Aeronomy of the Middle Atmosphere, Second Edition. D. Reidel, Dordrecht, 1984

Brewer, A. W., Evidence for a world circulation provided by the measurements of helium and water vapour distribution in the stratosphere, *Quart.J.R.Met.Soc.*, **75**, 351-363, 1949.

Burch, D. E., Continuum absorbtion by atmospheric H2O, *Proc. SPIE Atmos. Trans*., **277**, 28-37, 1981

Chiou E. W., M. P. McCormick, and W. P. Chu, Global water vapor distributions in the stratosphere and upper troposphere derived from 5.5 years of SAGE II observations (1986-1991), *J. Geophys. Res*., **102** (D15), 19105-19118, 1997

Cornford, S. G. and C. S. Spavins, Some measurements of cumulonimbus tops in pre-monsoon season in northeast india, *Meteorol.Mag.*, **102**(1216), 314-332, 1973.

Danielsen, E. F., A dehydration mechanism for the stratosphere, *Geophys.Res.Lett.*, **9**, 605-608, 1982.

Danielsen, E. F., In situ Evidence of Rapid, Vertical, Irreversible Transport of Lower Tropospheric Air Into the Lower Tropical Stratosphere by Convective Cloud Turrets and by Larger-Scale Upwelling in Tropical Cyclone, *J.Geophys.Res.*, **98**, 8665-8681, 1993.

Dessler, A. E. and H. Kim, Determination of the amount of water vapor entering the stratsphere based on Halgen Occultation Experiment (HALOE) data, *J.Geophys.Res.*, 104, 30605-30607, 1999.

Dessler, A. E. and H. Kim, Determination of the amount of water vapor entering the stratsphere based on Halgen Occultation Experiment (HALOE) data, *J.Geophys.Res.*, 104, 30605-30607, 1999.

Dessler, A. E., E. M. Weinstock, E. J. Hintsa, J. G. Anderson, C. R. Webster, R. D. May, J. W. Elkins, and G. S. Dutton, An examination of the total hydrogen budget of the lower stratosphere, *Geophys.Res.Lett.*, **21** (23), 2563-2566, 1994.

Dessler, A. E., The effect of deep, tropical convection on the tropical tropopause layer, *J.Geophys.Res.* , **107** (D3), 10.1029/2001JD000511, 2002.

Ebert, E. E. and G. J. Holland. Observations of record cold cloud-top temperatures in tropical cyclone Hilda-1990, *Mon. Weather Rev*., **120**, 2240-2251, 1992

Engel Al, C. Schiller, U. Schmidt, R. Borchers, H. Ovarlez, and J. Ovarlez, The total hydrogen budget in the Arctic winter stratosphere during the European Arctic Stratospheric Ozone Experiment, *J. Geophys. Res*., **101** (D9), 14495-14503, 1996

Evans, S. J., R. Toumi, J. E. Harries, and M. E. Chipperfield, Trends in stratospheric humidity and the sensitivity of ozone to these trends, *J. Geophys. Res*., **103**, 8715-8725, 1998

Folkins, I., K. K. Kelly, and E. M. Weinstock, A simple explanation for the increase in relative humidity between 11 and 14 km in the tropics, *J.Geophys.Res.*, 107(0), doi:10.1029/2002JD002185, 2002.

Folkins, I., M. Loewenstein, J. Podolske, J. Oltmans, and M. Proffitt, A barrier to vertical mixing at 14 km in the trpics: Evidence from ozonesondes and aircraft measurements, *J.Geophys.Res.*, **104**, 22,095-22,102, 1999.

Folkins, I., S. J. Oltmans, and A. M. Thompson, Tropical convective outflow and near surface equivalent potential temperatures, *Geophys.Res.Lett.*, **27**, 2549-2552, 2000.

Forster, P. M. de F. and K. P. Shine, Stratospheric water vapour changes as a possible contributor to observed stratospheric cooling, *Geophys. Res. Lett*., **26**, 3309-3312, 1999

Fritsch, J. M. and J. M. Brown, On the generation of convectively driven mesohighs aloft, *Mon.Wea.Rev.*, **110**, 1554-1563, 1982.

Fu, Q. and K. N. Liou, Parameterization of the Radiantive Properties of Cirrus Clouds, *J.Atmos.Sci.*, **50**, 2008-2025, 1993.

Gettelman, A., M. L. Salby, and F. Sassi, The distribution and influence of convection in the tropical tropopause region, *J.Geophys.Res.*, 107 (D10), doi:10.1029/2001JD001048, 2002.

Goody, R., Atmospheric Radiation, Theoretical Bases, Oxford University Press, 1964

Hansen A. R. and G. D. Robinson, Water-Vapor And Methane In The Upper-Stratosphere - An Examination Of Some Of The Nimbus-7 Measurements, *J. Geophys. Res*., **94** (D6), 8474-8484, 1989

Hartmann, D. L., J. R. Holton, and Q. Fu, The heat balance of the tropical tropopause, cirrus, and stratospheric dehydration, *Geophys.Res.Lett.*, **28**(10), 1969-1972, 2001.

Held, I. M., On the height of the tropopause and the static stability of the troposphere, *J. Atmos. Sci*., **39**(2), 412-41, 1982

Highwood, E. J. and B. J. Hoskins, The tropical tropopause, *Quart.J.R.Met.Soc.*, **124**, 1579-1604, 1998.

Hunt, G. E., Radiative properties of terrestrial clouds at visible and infra-red thermal window wavelengths, *Quart.J.R.Met.Soc.*, **99**, 346-369, 1973.

Hurst, D. F., G. S. Dutton, P. A. Romashkin, P. R. Wamsley, F. L. Moore, J. W. Elkins, E. J. Hintsa, E. M. Weinstock, R. L. Herman, E. J. Moyer, D. C. Scott, R. D. May, and C. R. Webster, Closure of the total hydrogen budget of the northern extratropical lower stratosphere, *J.Geophys.Res.*, **104** (D7), 8191-8200, 1999

Jensen, E. J., O. B. Toon, L. Pfister, and H. B. Selkirk, Dehydration of the upper troposphere and lower stratosphere bysubvisible cirrus clouds near the tropical tropopause, *Geophys. Res. Lett*., **23**, 825-828, 1996

Johnson, R. H. and D. C. Kriete, Thermodynamic and Circulation Characteristics of Winter Monsoon Tropical Mesoscale Convection, *Mon.Wea.Rev.*, **110**(12), 1898-1911, 1982.

Johnston, H. S. and S. Solomon, Thunderstorms as possible micrometeorological sink for stratospheric water, *J.Geophys.Res.*, **84**, 3155-3158, 1979.

Jones, R. L., J. A. Pyle, J. E. Harries, A. M. Zavody, J. M. Russell III, and J. C. Gille, The water vapor budget of the stratosphere studied using LIMS and SAMS satellite data, *Q. J. R. Meteorol. Soc*., **112**, 1127-1143, 1986

Kalnay, E., M. Kanamitsu, R. Kistler, W. Collins, D. Deaven, L. Gandin, M. Iredell, S. Saha, C. White, J. Woollen, Y. Zhu, M. Chelliah, W. Ebisuzaki, W. Higgins, J. Janowiak, K. C. Mo, C. Ropelewski, J. Wang, A. Leetmaa, R. Reynolds, P. Jenne, and D. Joseph, The NCEP/NCAR 40-year reanalysis project, *Bull.Amer.Meteor.Soc.*, **77**, 437-471, 1996.

Keith, D. W., Stratosphere-troposphere exchange: Inferences from the isotopic composition of water vapor, *J. Geophys. Res*., **105** (D12), 15167-15173, 2000

Kelly K. K., A. F. Tuck, L. E. Heidt, M. Lewenstein, J. R. Podolske, S. E. Strahan, and J. F. Vedder, A Comparison Of Er-2 Measurements Of Stratospheric Water-Vapor

Between The 1987 Antarctic And 1989 Arctic Airborne Missions, *Geophys. Res. Lett*., **17** (4), 465-468, 1990

Kidder, S. Q. and T. H. Vonder Haar, Satellite Meteorology, Academic Press Inc., 1995.

Kiladis, G. N., K. H. Straub, G. C. Reid, and K. S. Gage, Aspects of interannual and intraseasonal variability of the tropopause and lower stratosphere, *Q. J. R. Meteorolo. Soc*., **127** (576), 1961-1983, 2001

Kirk-Davidoff, D. B., E. J. Hintsa, J. G. Anderson, and D. W. Keith, The effect of climate change of ozone depletion through changes in stratospheric water vapor, *Nature*, **402**, 399-401, 1999

Kley, D., E. J. Stone, W. R. Henderson, J. W. Drummond, W. J. Harrop, A. L. Schmeltekopf, T. L. Thompson, and R. H. Winkler, In situ measurements of the mixing ratio of water vapor in the stratosphere, *J. Atmos. Sci*., **36**, 2513-2524, 1979

Knollenberg R. G., A. J. Dascher, and D. Huffman, Measurements of the aerosol and ice crystal populations in tropical stratospheric cumulonimbus anvils, *Geophys. Res. Lett*., **9** (6), 613-616, 1982

Kritz, M. A., S. W. Rosner, K. K. Kelly, M. Loewenstein, and K. R. Chan, Radon Measurements in the Lower Tropical Stratosphere: Evidence for Rapid Vertical Transport and Dehydration of Tropospheric Air, *J.Geophys.Res.*, **98**, 8725-8736, 1993.

Kuang, Z. and C. S. Bretherton, Convective influence on the heat balance of the tropical tropopause layer: A cloud-resolving model study, *J.Atmos.Sci.*, submitted , 2004.

Kummerow, C., W. Barnes, T. Kozu, J. Shine, and J. Simpson, The Tropical Rainfall Measuring Mission (TRMM) Sensor Package, *J.Atmos.and Oceanic Tech.*, **15**(3), 809-817, 1998.

LeTexier, H., S. Solomon, and R. R. Garcia, The role of molecular hydrogen and methane oxidation in the water vapor budget of the stratosphere, *Q. J. R. Meteorolo. Soc.,***114**, 281-295, 1988

Michelsen, H. A., F. W. Irion, G. L. Manney, G. C. Toon, and M. R. Gunson, Features and trends in ATMOS version 3 water vapor and methane measurements, *J.Geophys.Res.*, **105**, 22713-22722, 2000.

Mote, P. W., K. H. Rosenlof, J. R. Holton, R. S. Harwood, and J. W. Waters, Seasonal-variations of water-vapor in the tropical lower stratosphere, *Geophys.Res.Lett.*, 22 (9), 1093 – 1096, 1995

Mote, P. W., K. H. Rosenlof, M. E. McIntyre, E. S. Carr, J. C. Gille, J. R. Holton, J. S. Kinnersley, H. C. Pmphrey, J. M. Russell, J. W. Waters, An atmospheric tape recorder: The imprint of tropical tropopause temperatures on stratospheric water vapor, *J.Geophys.Res.*, **101** (D2): 3989-4006, 1996

Nedoluha, G. E., R. M. Bevilacqua, R. M. Gomez, D. E. Siskind, B. C. Hicks, and J. M. Russell III, Increases in middle atmospheric water vapor as observed by the Halogen Occultation Experiment (HALOE) and the ground-based Water Vapor Millimeter-wave Spectrometer from 1991-1997, *J. Geophys.Res*., **103**, 3531-3542, 1998

Negri, A. J., Cloud-top structure of tornadic storms on 10 April 1979 from rapid scan and stereo satellite observations, *Bull.Amer.Meteor.Soc.*, **63**, 1151-1159, 1982.

Newell, R. E., and S. Gould-Stewart, A stratospheric fountain?, *J. Atmos. Sci*., **38**, 2789-2796, 1981

Newton, C. W., and A. V. Persson, Structural Characteristics of The Subtropical Jet Stream And Certain Lower-Stratospheric Wind Systems, *Tellus*, **14** (2), 221-241, 1962

Oltmans S. J. and D. J. Hofmann, Increase In Lower-Stratospheric Water-Vapor At A Mid-Latitude Northern-Hemisphere Site From 1981 To 1994, *Nature*, **374** (6518), 146-149, 1995

Oltmans S. J., H. Vomel, D. J. Hofmann, K. H. Rosenlof, and D. Kley, The increase in stratospheric water vapor from balloonborne, frostpoint hygrometer measurements at Washington, DC, and Boulder, Colorado, *Geophys. Res. Lett*., **27** (21), 3453-3456, 2000

Ou, S. C., K. N. Liou, W. M. Gooch, and Y. Takano, Remote sensing of cirrus cloud parameters using advanced very-high-resolution radiometer 3.7- and 10.9-m channels, *Appli.Optics*, **32**(12), 2171-2180, 1993.

Pfister, L., Small-scale motions observed by aircraft in the tropical lower stratosphere: evidence for mixing and its relationship to large-scale flows, *J. Atmos. Sci*., **43**(24), 3210-3225, 1986

Potter, B. E. and J. R. Holton, The role of monsoon convection in the dehydration of the lower tropical stratosphere, *J.Atmos.Sci.*, **52**(8), 1034-1050, 1995.

Randel W. J., F. Wu, and D. J. Gaffen, Interannual variability of the tropical tropopause derived from radiosonde data and NCEP reanalyses, *J. Geophys. Res*., **105** (D12), 15509-15523, 2000

Randel, W. J., F. Wu, and W. Rivera Rios, Thermal variability of the tropical tropopause region derived from GPS/MET observations, *J.Geophys.Res.*, **108** (D1), 4024, doi:10.1029/2002JD002595, 2003.

Reid G. C. and K. S. Gage, Interannual Variations In The Height Of The Tropical Tropopause, *J. Geophys. Res*., **90** (ND3), 5629-5635, 1985

Reid G. C. and K. S. Gage, On The Annual Variation In Height Of The Tropical Tropopause. *J. Atmos. Sci*., **38** (9), 1928-1938, 1981

Robinson G. D., The Transport Of Minor Atmospheric Constituents Between Troposphere And Stratosphere, *Q. J. R. Meteorolo. Soc*., **106** (448), 227-253, 1980

Rosenfeld, D. and I. M. Lensky, Satellite-Based Insights into Precipitation Formation Processes in Continental and Maritime Convective Clouds, *Bull.Amer.Meteor.Soc.*, **79**, 2457-2479, 1998.

Selkirk H. B., The Tropopause Cold Trap In The Australian Monsoon During Step Amex 1987, *J. Geophys. Res*., **98** (D5), 8591-8610, 1993

Sherwood S. C., Aerosols and ice particle size in tropical cumulonimbus, *J. Climate*, **15** (9), 1051-1063, 2002

Sherwood, S. C. and A. E. Dessler, A model for transport across the tropical tropopause, *J.Atmos.Sci.*, **7**, 765-779, 2001.

Sherwood, S. C. and A. E. Dessler, On the control of stratospheric humidity, *Geophys.Res.Lett.*, **27** (16), 2513-2516, 2000.

Sherwood, S. C. and R. Warhlich, Observed evolution of tropical deep convective events and their environment, *Mon.Wea.Rev.*, **127** (8), 1777-1795, 1999.

Sherwood, S. C., A stratospheric "drain" over the maritime continent, *Geophys.Res.Lett.*, **27** (5), 677-680, 2000.

Sherwood, S. C., Aerosols and Ice Particle Size in Tropical Cumulonimbus, *J.Climate*, **15** (9), 1051-1063, 2002.

Sherwood, S. C., T. Horinouchi, and H. A. Zeleznik, Convective impact on temperatures observed near the tropical tropopause, *J.Atmos.Sci.*, **60**(15), 1847-1856, 2003.

Shindell D. T., Climate and ozone response to increased stratospheric water vapor, *Geophys. Res. Lett*., **28** (8), 1551-1554, 2001

Simmons A. J., A. Untch, C. Jakob, P.Kallberg, and P. Unden, Stratospheric water vapour and tropical tropopause temperatures in ECMWF analyses and multi-year simulations, *Q. J. R. Meteorolo. Soc*., **125** (553), 353-386, 1999

Simpson J., J. B. Halverson, B. S. Ferrier, W. A. Petersen, R. H. Simpson, R. Blakeslee, and S. L. Durden, On the role of "hot towers" in tropical cyclone formation, *Meteorol. And Atmos. Phys*., **67** (1-4), 15-35, 1998

Simpson, J., C. Kummerow, W. K. Tao, and F. A. Adler, On the tropical rainfall measuring mission (TRMM), *Meteorology and Atmospheric physics*, **60**(1-3), 19-36, 1996.

SPARC, Kley, D., Russell III, J. M., and Phillips, C. SPARC Report on Distribution and Variability of Water Vapour in the Upper Troposphere and Lower Stratosphere, in SPARC Assessment of Upper Tropospheric and Stratospheric Water Vapour (WMO/TD-No. 1043). WCRP-113. 2000.

Stenke A. and V. Grewe, Impact of dynamically induced ozone mini-hole events on PSC formation and chemical ozone destruction, *Climate Change Processes In The Stratosphere, Earth-Atmosphere-Ocean Systems, And Oceanographic Processes From Satellite Data Advances In Space Research*, **33** (7),1062-1067, 2004

Stowasser M., H. Oelhaf, G. Wetzel, F. Friedl-Vallon, G. Maucher, N. Seefeldner, O. Trieschmann, T. Von Clarmann, and H. Fischer, Simultaneous measurements of HDO, H2O, and CH4 with MIPAS-B: Hydrogen budget and indication of dehydration inside the polar vortex, J. Geophys. Res., 104 (D16), 19213-19225, 1999

Thuburn, J. and G. C. Craig, Stratospheric influence on tropopause height: The radiative constraint, *J. Atmos. Sci*., **57** (1), 17-28, 2000

Tsuda T., Y. Murayama, H. Wiryosumarto, S. W. B. Harijono, and S. Kato, Radiosonde Observations Of Equatorial Atmosphere Dynamics Over Indonesia .1. Equatorial Waves And Diurnal Tides, *J. Geophys. Res*., **99** (D5), 10491-10505, 1994

van Hees, R. M. and J. Lelieveld, Retrieving cloud top structure from infrared satellite data, *J.Geophys.Res.*, **105**, 15,663-15,671, 2000.

Wayne, R. P., Chemistry of Atmospheres, Oxford University Press, 1985

Wennberg P. O., et al., Removal Of Stratospheric O-3 By Radicals - In-Situ Measurements of OH, HO2, NO, NO2, CLO, and BRO, *Science*, **266** (5184), 398-404, 1994

Winker D. M. and C. R. Trepte, Laminar cirrus observed near the tropical tropopause by LITE, *Geophys. Res. Lett*., **25** (17), 3351-3354, 1998

Zhou X. L., M. A. Geller, and M. H. Zhang, Cooling trend of the tropical cold point tropopause temperatures and its implications, *J. Geophys. Res*., **106** (D2), 1511-1522, 2001

Zőger, M., A. Engel, D. S. McKenna, C. Schiller, U. Schmidt, and T. Woyke, Balloon-borne in situ measurements of stratospheric H_{2O}, *J.Geophys.Res.*, **104** (D1), 1817-1825, 1999